

# Biofabrication Strategies for Oral Soft Tissue Regeneration

Maedeh Rahimnejad, Hardik Makkar, Renan Dal-Fabbro, Jos Malda, Gopu Sriram,\*  
and Marco C. Bottino\*

Gingival recession, a prevalent condition affecting the gum tissues, is characterized by the exposure of tooth root surfaces due to the displacement of the gingival margin. This review explores conventional treatments, highlighting their limitations and the quest for innovative alternatives. Importantly, it emphasizes the critical considerations in gingival tissue engineering leveraging on cells, biomaterials, and signaling factors. Successful tissue-engineered gingival constructs hinge on strategic choices such as cell sources, scaffold design, mechanical properties, and growth factor delivery. Unveiling advancements in recent biofabrication technologies like 3D bioprinting, electrospinning, and microfluidic organ-on-chip systems, this review elucidates their precise control over cell arrangement, biomaterials, and signaling cues. These technologies empower the recapitulation of microphysiological features, enabling the development of gingival constructs that closely emulate the anatomical, physiological, and functional characteristics of native gingival tissues. The review explores diverse engineering strategies aiming at the biofabrication of realistic tissue-engineered gingival grafts. Further, the parallels between the skin and gingival tissues are highlighted, exploring the potential transfer of biofabrication approaches from skin tissue regeneration to gingival tissue engineering. To conclude, the exploration of innovative biofabrication technologies for gingival tissues and inspiration drawn from skin tissue engineering look forward to a transformative era in regenerative dentistry with improved clinical outcomes.

## 1. Introduction

Gingival recession, characterized by the exposure of tooth roots due to the loss of protective gingival tissues, is a widespread issue affecting nearly half of all adults in the United States.<sup>[1–3]</sup> This common condition poses oral health challenges and diminishes the quality of life for millions. Patients with gingival recession often face discomfort, a heightened risk of bacterial biofilm development, aesthetic concerns, and root sensitivity, particularly during chewing. Tissue loss is triggered mainly by periodontitis-related inflammation (following innate immune response to bacterial plaque/biofilm and bacterial products) and mechanical stress.<sup>[2–4]</sup> When gingival recession progresses to an advanced stage, the exposed tooth roots become susceptible to cariogenic bacteria, potentially leading to root caries and, in severe cases, tooth loss.<sup>[2–4]</sup> Addressing this pervasive issue demands effective periodontal plastic surgical treatments that reduce patient discomfort and restore healthy gingival tissues.

Preimplant surgical reconstruction is crucial in addressing various issues, such as gingival recession and insufficient tissue around the tooth.<sup>[7]</sup> The primary motivation

M. Rahimnejad, R. Dal-Fabbro, M. C. Bottino  
Department of Cariology  
Restorative Sciences  
and Endodontics  
School of Dentistry  
University of Michigan  
Ann Arbor, MI 48109, USA  
E-mail: [mbottino@umich.edu](mailto:mbottino@umich.edu)

H. Makkar, G. Sriram  
Faculty of Dentistry  
National University of Singapore  
Singapore 119085, Singapore  
E-mail: [sriram@nus.edu.sg](mailto:sriram@nus.edu.sg)

J. Malda  
Regenerative Medicine Center Utrecht  
Utrecht 3584, The Netherlands

J. Malda  
Department of Clinical Sciences  
Faculty of Veterinary Medicine  
Utrecht University  
Utrecht 3584, The Netherlands

J. Malda  
Department of Orthopedics  
University Medical Center Utrecht  
Utrecht 3584, The Netherlands

 The ORCID identification number(s) for the author(s) of this article can be found under <https://doi.org/10.1002/adhm.202304537>

© 2024 The Authors. Advanced Healthcare Materials published by Wiley-VCH GmbH. This is an open access article under the terms of the [Creative Commons Attribution-NonCommercial](https://creativecommons.org/licenses/by-nc/4.0/) License, which permits use, distribution and reproduction in any medium, provided the original work is properly cited and is not used for commercial purposes.

DOI: [10.1002/adhm.202304537](https://doi.org/10.1002/adhm.202304537)

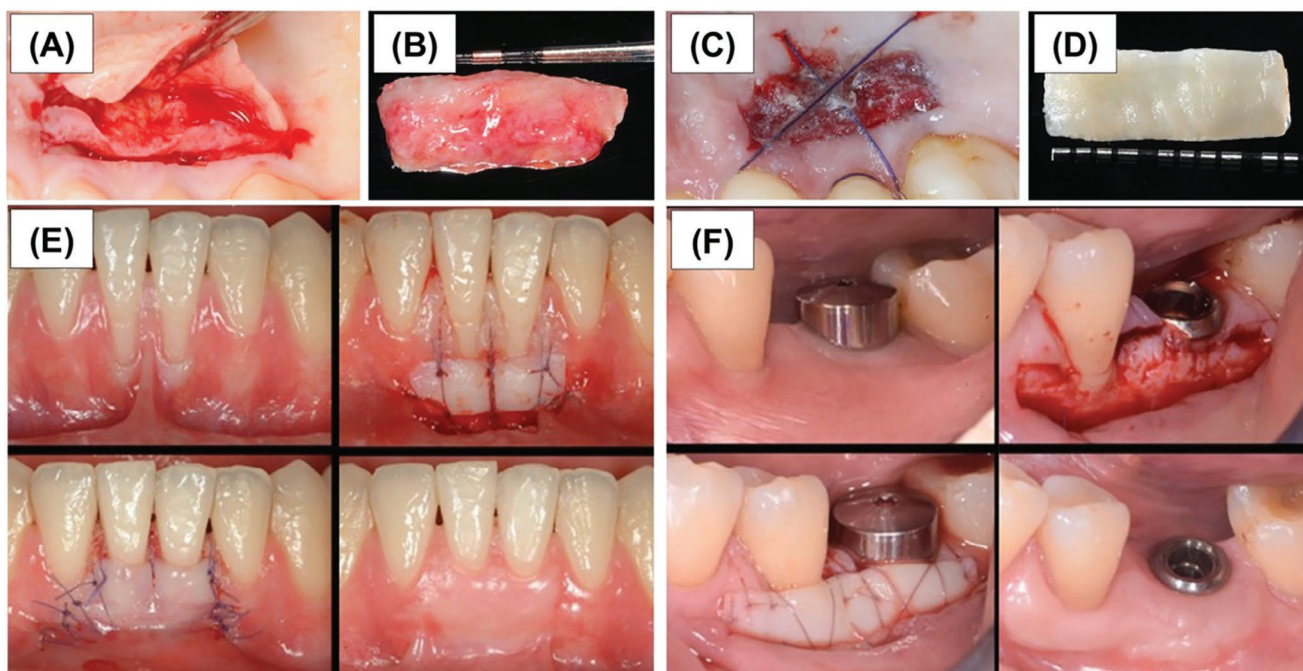


**Figure 1.** The current standard of care for soft tissue reconstruction around teeth and dental implants. A,B) Subepithelial connective tissue graft harvested using the Trapdoor technique, C,D) Free gingival graft harvested from the hard palate, reprinted under term of the Creative Commons CC-BY-NC-ND license,<sup>[5]</sup> E) Free gingival graft used to treat the gingival recession involving the mandibular central incisors, and its post-operative engraftment and healing, and F) Free gingival graft placed around a dental implant in the posterior molar region to enhance the width of keratinized mucosa on the buccal aspect, adapted from,<sup>[6]</sup> Copyright 2019, John Wiley and Sons.

behind this requirement is to achieve an ideal amount of gum and bone to support surrounding restorations or implants. Hard and soft tissue reconstruction may be necessary to create a stable foundation for successful implant placement and restoration.<sup>[4]</sup> The current standard of care for gingival recession and associated soft tissue defects typically involves periodontal plastic surgery techniques. These techniques often utilize autologous soft tissue grafts, including free gingival grafts (FGGs) and connective tissue grafts (CTGs), harvested from the patient's palate. Additionally, procedures such as coronally advanced flaps and pedicle grafts may be employed, utilizing gingival tissues from either the same tooth or an adjacent one (Figure 1A–D).<sup>[5,8]</sup> Zucchelli et al. recently reviewed these clinical approaches.<sup>[6]</sup> One of the clinical techniques mentioned in periodontal plastic surgery studies following the 2015 AAP Regeneration Workshop is the free gingival graft (FGG), as shown in Figure 1E,F.<sup>[6]</sup> The FGG was initially

utilized to repair keratinized tissue that had become deficient or lost during development. Several risk factors for FGG have been reported, including but not limited to inadequate recipient site preparation, insufficient graft size and thickness, poor adaptation to the recipient bed, and graft instability.<sup>[7]</sup> Because FGG shrinks substantially ( $\approx 30\%$ ) throughout the healing procedure, a graft larger than the zone requiring soft tissue replacement must be collected, which may explain the donor site's postoperative discomfort and complications.<sup>[7]</sup> Enough keratinized tissue breadth and thickness seems crucial for natural teeth and dental implants. Furthermore, marginal bone loss has been associated with peri-implant soft tissue thickness.<sup>[7]</sup>

The transition from free gingival graft (FGG) to connective tissue graft (CTG) signifies a shift from the traditional mucogingival surgical technique to the more advanced field of periodontal plastic surgery.<sup>[9]</sup> While conventional mucogingival methods' primary focus was expanding the keratinized tissue's width (KTW), the primary focus of contemporary periodontics should be on the final aesthetic results. Extensive studies have shown that a CTG is the most effective approach for healing gingival and mucosal recessions at tooth and implant sites, enhancing soft tissue thickness, covering exposed roots and implant parts, and reconstructing interdental papillae.<sup>[6]</sup> The coronally advanced flap (CAF), lateral rotational flap, semilunar flap, tunnel technique, and vestibular incision subperiosteal tunnel access (VISTA) approach are a few of the methods that have been developed for treating gingival recessions using a CTG or a graft replacement.<sup>[6]</sup> CTG-based therapies have the most significant promise to obtain full root coverage and improved aesthetics. During the first stages

G. Sriram  
NUS Centre for Additive Manufacturing (AM.NUS)  
National University of Singapore  
Singapore 117597, Singapore

G. Sriram  
Department of Biomedical Engineering  
National University of Singapore  
Singapore 117583, Singapore

M. C. Bottino  
Department of Biomedical Engineering  
College of Engineering  
University of Michigan  
Ann Arbor, MI 48109, USA

**Table 1.** The comparison of free gingival graft (FGG) and connective tissue graft (CTG) methods, including their success rate and limitations.<sup>[10–11]</sup>

Features	Free gingival graft (FGG)	Connective tissue graft (CTG)
Donor Tissue Source	Palate (roof of the mouth)	Palate (subepithelial layer)
Indication	Gingival recession	Gingival recession, root coverage
Tissue Type	Full-thickness gingival tissue	Subepithelial connective tissue
Graft Design	Epithelium and connective tissue	Only connective tissue
Graft Size	Limited to the size of the donor site	Limited to the size of the donor site
Wound Closure	Sutured	Sutured
Healing Outcome	Increased width of keratinized tissue	Increased width of keratinized tissue, root coverage
Esthetic Outcome	Moderate esthetic outcome	Excellent esthetic outcome
Post-operative Discomfort	Palatal discomfort and pain	Palatal discomfort and pain
Graft Success Rate	Generally high success rate	Generally high success rate
Potential Complications	Graft shrinkage, graft failure, color mismatch	Graft shrinkage, graft failure, color mismatch

of wound healing, the CTG may serve as a biological filler, enhancing the adaptability and stability of the flap to the root.<sup>[6]</sup> This transition is associated with an increased likelihood of achieving complete root coverage and an augmentation of the gingival phenotype thickness. However, it has been shown that patient discomfort and pain are similar to the FGG method.<sup>[6]</sup> **Table 1.** shows the differences between FGG and CTG and their limitations.

Although autologous grafts have been extensively utilized clinically for periodontal plastic surgery, they still carry fundamental issues related to donor site morbidity, tissue shortage and retention, and site-specific characteristics of the tissue. This has led to the exploration of alternate strategies for gingival recession management. Past work in the early 1980s demonstrated the use of cultured epithelial cell sheets of human skin and mucosa for intraoral grafting.<sup>[12]</sup> However, these sheets lacked tissue architecture and underlying supporting structures, making them fragile and challenging to handle. With the advances in tissue engineering in the past two decades, alternative approaches have been realized toward the biofabrication of gingival tissue constructs. This can be seen in using and validating tissue-engineered oral mucosa and gingival equivalents for fundamental research,<sup>[13–14]</sup> translational applications in animal models, and limited proof-of-concept use in clinical studies for oral and extraoral applications.<sup>[14–20]</sup> Breaking the regulatory barriers, allogeneic cultured keratinocytes and fibroblasts in bovine collagen (Organogenesis' GINTUIT) became the first regenerative dentistry product that secured FDA approval in 2012 for treating mucogingival defects in adult patients and is applied topically to surgically prepared vascular gingival graft bed.<sup>[21]</sup>

In contrast to conventional methods, 3D bioprinting technology facilitates the creation of tissues through a systematic and reproducible layer-by-layer assembly process. This innovative approach enables the precise construction of tissues or even entire organs, offering potential breakthroughs in regenerative medicine and transplantation. Unlike 3D bioprinting, perfusion-based microfluidic organ-on-chip systems primarily serve as advanced disease modeling and drug discovery platforms. These systems leverage microfluidic principles to mimic the physiological conditions of human organs, aiding in the study of disease mechanisms and the evaluation of therapeutic interventions.<sup>[22–23]</sup> Integrating these technological advance-

ments with a deep understanding of advanced materials and engineered constructs holds substantial promise for enhancing current clinical approaches to gingival regeneration, offering personalized interventions, expedited recovery, and minimized surgical interventions.<sup>[14–17,24]</sup> Though tissue engineering is in its early stages for periodontal regenerative therapies, it holds significant promise. This review explores alternative biofabrication strategies for overcoming challenges in traditional mucogingival treatments, outlining critical considerations for gingival tissue construct biofabrication. Lastly, we focus on exploring alternative biofabrication strategies, including insights from skin biofabrication and regeneration approaches, on further expanding the potential for cross-application in gingival tissue regeneration.

## 2. Gingiva and Oral Mucosa

The major soft tissue component of the mouth is the oral mucosa, which includes the gingiva (commonly referred to as gums) and mucosal tissue that lines other parts of the oral cavity, including the alveolar bone, palate, tongue, floor of the mouth, cheeks, and the lips. Gingiva and oral mucosa serve as a barrier, shielding the deeper oral tissues from the environmental conditions within the oral cavity. Everyday activities such as grasping, biting, and chewing food subject the soft tissues of the mouth to mechanical stresses, including compression, stretching, shearing, and surface abrasions caused by rigid dietary particles. The oral mucosa exhibits numerous adaptations in its epithelial and connective tissue components to withstand these challenges. Moreover, the sensory function of the oral mucosa holds paramount significance, serving as a vital source of information concerning the dynamic processes occurring in the oral cavity. In this unique environment, specialized receptors play a crucial role by detecting changes in temperature, registering tactile sensations, and signaling pain, thereby facilitating the recognition and regulation of diverse stimuli and oral conditions.

Histologically, the oral mucosa primarily comprises two key tissue elements (**Figure 2**): a stratified squamous epithelium, referred to as the oral epithelium, and a connective tissue layer beneath it known as the lamina propria.<sup>[25]</sup> Both components orchestrate the responses associated with developing gingival health and disease. The mucosa in areas subjected to mechanical stress (gingiva and hard palate), called masticatory mucosa,

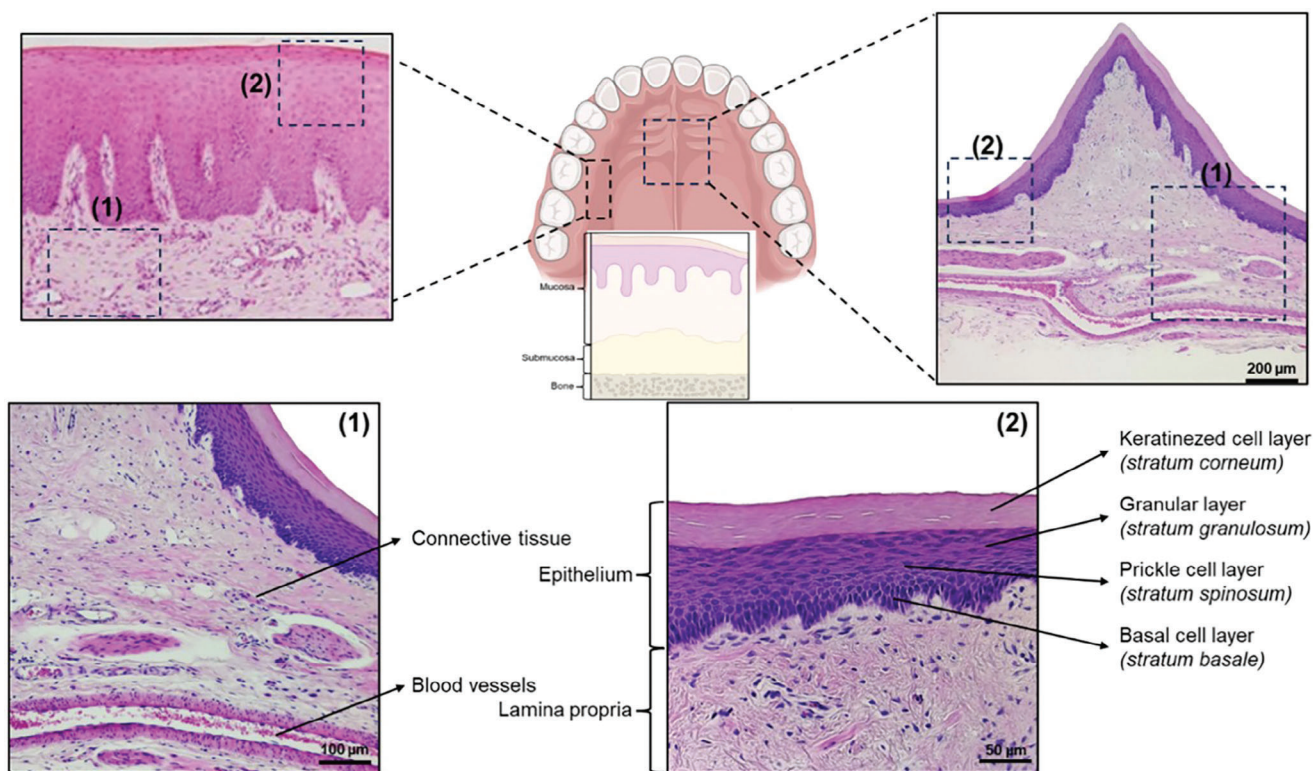


**Figure 2.** Histomorphology of the human gingiva. Hematoxylin and eosin (H&E) stained the histological section of the hard palate and gingival tissue, showing the different tissue structures and cell layers. Some of the H&E images are adapted from<sup>[26]</sup> Copyright 2013, PubMed.

is lined by a keratinized stratified squamous epithelium. In contrast, the mucosa lining lines other parts of the oral cavity (alveolar bone, palate, tongue, floor of the mouth, cheeks, and lips), referred to as lining mucosa, is covered by nonkeratinized stratified squamous epithelium that is devoid of the corneal layer.<sup>[26]</sup>

Owing to the high mechanical forces from chewing, the masticatory mucosa is characterized by its rigidity, resilience to abrasion, keratinized epithelium, and firm adherence to the underlying lamina propria. The basal layer of the epithelium, also known as the *stratum basale*, consists of cuboidal cells adjacent to the basement membrane.<sup>[27]</sup> Positioned above the basal layer are multiple rows of larger polygonal cells called the prickle cell layer or *stratum spinosum*. This terminology is derived from their appearance in histological preparations, where they appear to separate from each other, maintaining contact only at specific points known as intercellular bridges or desmosomes.<sup>[28]</sup> The basal and prickle cell layers contribute to approximately one-half to two-thirds of the epithelium's total thickness. Moving upwards, the subsequent layer comprises larger flattened cells containing small granules that exhibit intense staining with acid dyes such as hematoxylin. This layer is identified as granular or *stratum granulosum*.<sup>[25]</sup> Finally, the outermost layer comprises flat (squamous) cells, known as *squames*, which exhibit vivid pink staining with the histological dye eosin, appearing eosinophilic, and do not contain any nuclei. This uppermost layer is referred to as the keratinized layer or *stratum corneum*.<sup>[26]</sup>

The junction between the oral epithelium and the connective tissue of the lamina propria is a dynamic interface characterized

by the undulating interlocking of the epithelial ridges and connective tissue papillae. This unique configuration enhances the surface area of the interface compared to a simple, flat junction, facilitating a stronger attachment and allowing forces applied to the epithelium's surface to be distributed over a larger region of connective tissue. The lamina propria serves as the supportive connective tissue for the oral epithelium. This intricate structure comprises various elements, including cells, blood vessels, neural elements, and extracellular matrix fibers embedded within an unstructured ground substance rich in water, glycosaminoglycans, proteoglycans, glycoproteins, and other molecules. The cellular composition of lamina propria encompasses fibroblasts, mesenchymal stem cells, macrophages, mast cells, and inflammatory cells, with the fibroblast being the most common cell type. Fibroblasts play a crucial role in preserving the oral mucosa's lamina propria's structural integrity by producing and renewing the fibers and ground substance. In adult oral mucosa, fibroblasts have a relatively low proliferation rate except when triggered during wound healing.<sup>[29–31]</sup>

Furthermore, the oral mucosa boasts a robust blood supply, primarily sourced from arteries coursing alongside the mucosal surface within the submucosal layer. In cases where the mucosa tightly adheres to the underlying periosteum and the submucosal layer is absent, these arteries can be found in the deeper portion of the reticular layer. From these main arteries, smaller branches emanate and connect with neighboring vessels within the reticular layer, eventually forming an intricate capillary network just beneath the basal epithelial cells in the papillary layer.<sup>[30]</sup>

The gingival epithelium can be categorized into three types based on the microanatomical location: oral, sulcular, and junctional epithelium. Briefly, the oral gingival epithelium covers the outer surface of the gingiva and extends from the free gingival margin to the mucogingival junction. The sulcular epithelium lines the gingival sulcus, extending from the gingival crest tip to the most coronal part of the junctional epithelium.<sup>[29–31]</sup> From here, the junctional epithelium extends from the base of the gingival sulcus to  $\approx 2$  mm coronal to the alveolar bone crest. It is closely adapted to the tooth surface and contributes towards sealing and attachment functions.<sup>[32]</sup> These subsets of the gingival epithelium differ histologically,<sup>[33]</sup> where the oral gingival epithelium exhibits features similar to keratinized epithelium.

In contrast, sulcular and junctional epithelium are similar to lining mucosa (nonkeratinized). They also differ in the expression of key cytokeratins (CK), especially the absence of CK13 and CK19 in the keratinized gingival epithelium and a high expression of CK19 across all layers of the junctional epithelium.<sup>[34–36]</sup> The three gingival epithelial linings play an integral role in tissue protection, homeostasis, and bidirectional movement of substances between the gingival connective tissue and the oral cavity and provide a gateway for the host immune defense to play an instructive and collaborative role in keeping the oral microbiome at bay. The egress of interstitial flow from the connective tissue into the gingival crevice, commonly called the gingival crevicular fluid, with its host protective function is well established.<sup>[37]</sup> Additionally, the metabolically active epithelial cells play an integral role in host protection by producing and transporting cytokines, antimicrobial peptides, and growth factors.<sup>[38–39]</sup>

### 3. Tissue Engineering and Biofabrication of Gingival Constructs

Recapitulating the intricate functionalities of gingival tissues *in vitro* presents a formidable challenge, necessitating a complex 3D microenvironment that cannot be provided by conventional monolayer cultures or acellular biomaterial-based approach. Progress in cell culture techniques, tissue engineering, and biofabrication strategies, driven by clinical demand to replace lost gingival tissues, limited availability to autologous tissues, and regulatory pressure to replace animal models with alternative testing methods, has spurred the development of 3D organotypic models of human gingiva. The demand for such biofabricated gingival constructs is substantial and holds profound implications in fundamental research and clinical therapeutic/regenerative applications.

Biofabrication, a rapidly evolving field in tissue engineering and regenerative medicine, involves precisely fabricating living constructs using advanced tissue engineering techniques. Several critical factors are pivotal in the successful biofabrication of functional tissues and organs.<sup>[40]</sup> The advancement of biofabrication technologies and understanding these vital factors are essential for successfully fabricating functional tissues and organs, paving the way for transformative applications in regenerative medicine and personalized healthcare. Here, we discuss some key biomaterial, cellular, and biological factors to be considered for incorporation with the various enabling biofabrication technologies (Figure 3).

#### 3.1. Biomaterial Considerations

##### 3.1.1. Porosity

The porosity of the biomaterial plays a crucial role in the effective regeneration of the biofabricated tissue. Scaffolds or implants with interconnected pores create a 3D structure closely mimicking the natural extracellular matrix (ECM) environment. This porous structure can offer several advantages for cell attachment and integration.<sup>[41]</sup> Porous materials have a larger surface area than nonporous materials of the same volume, as shown in Figure 4A. This expanded surface area provides more room for cell adhesion and spreading, allowing for better cell attachment. The interconnected pores facilitate the diffusion of oxygen, transfer of nutrients, and removal of waste products throughout the structure. This supports cell viability and functionality, especially in thicker tissue constructs. In addition, the increased porosity contributes to increased cellular metabolism and development by promoting enhanced nutrition, gas diffusion, and efficient waste disposal.<sup>[42–43]</sup>

The ECM is a dynamic and complex network of proteins, glycoproteins, proteoglycans, and other molecules that provide cells with structural support and vital metabolic signals. Biofabrication strategies with spatial organization capabilities enable the potential to create porous materials emulating the ECM structure and composition. The interconnected pores in a porous material can serve as pathways for cell migration and tissue ingrowth, facilitating the establishment of cell connections and promoting new tissue formation and integration with the host tissue. Optimal porosity enables early microvascular penetration, graft stabilization, and integration with the host tissue.<sup>[46–47]</sup> More specifically, macropores between 100 and 700  $\mu\text{m}$  promote blood vessel formation at the implanted locations, while micropores  $< 100$   $\mu\text{m}$  may hinder cell viability due to local ischemia.<sup>[47–48]</sup>

It is important to note that the specific porosity requirements may vary depending on the intended application, cell type, and tissue being targeted. Optimization of porosity, pore size, and pore interconnectivity is necessary to achieve the desired cell attachment, integration, and overall tissue regeneration outcomes. Many different approaches to fabrication have been employed to develop various porous scaffold designs.<sup>[49]</sup> Gingival connective tissue comprises two distinct regions: the papillary and reticular regions, each with unique characteristics and functions.<sup>[50]</sup> Each zone has a hierarchical structure, which can impact the porosity of the connective tissue. For instance, the papillary region, being superficial connective tissue, has thinner collagen fibers arranged irregularly. On the contrary, the reticular portion, the deeper section of the gingival connective tissue, has thicker collagen fibers arranged in a parallel orientation to the underlying mucoperiosteum.<sup>[51]</sup> To assess the suitability of pores while engineering soft tissues, *in vivo* models have been employed, monitoring tissue response, inflammation, and immune reactions longitudinally.<sup>[52]</sup> In parallel fashion, *in vitro* models have scrutinized cell proliferation and microvascularization, underscoring the critical role of porosity and specific pore sizes.

Advanced microscopy techniques, including scanning electron microscopy (SEM), transmission electron microscopy (TEM), atomic force microscopy (AFM), and BET (Brunauer–Emmett–Teller) analysis, offer enhanced insights to devise

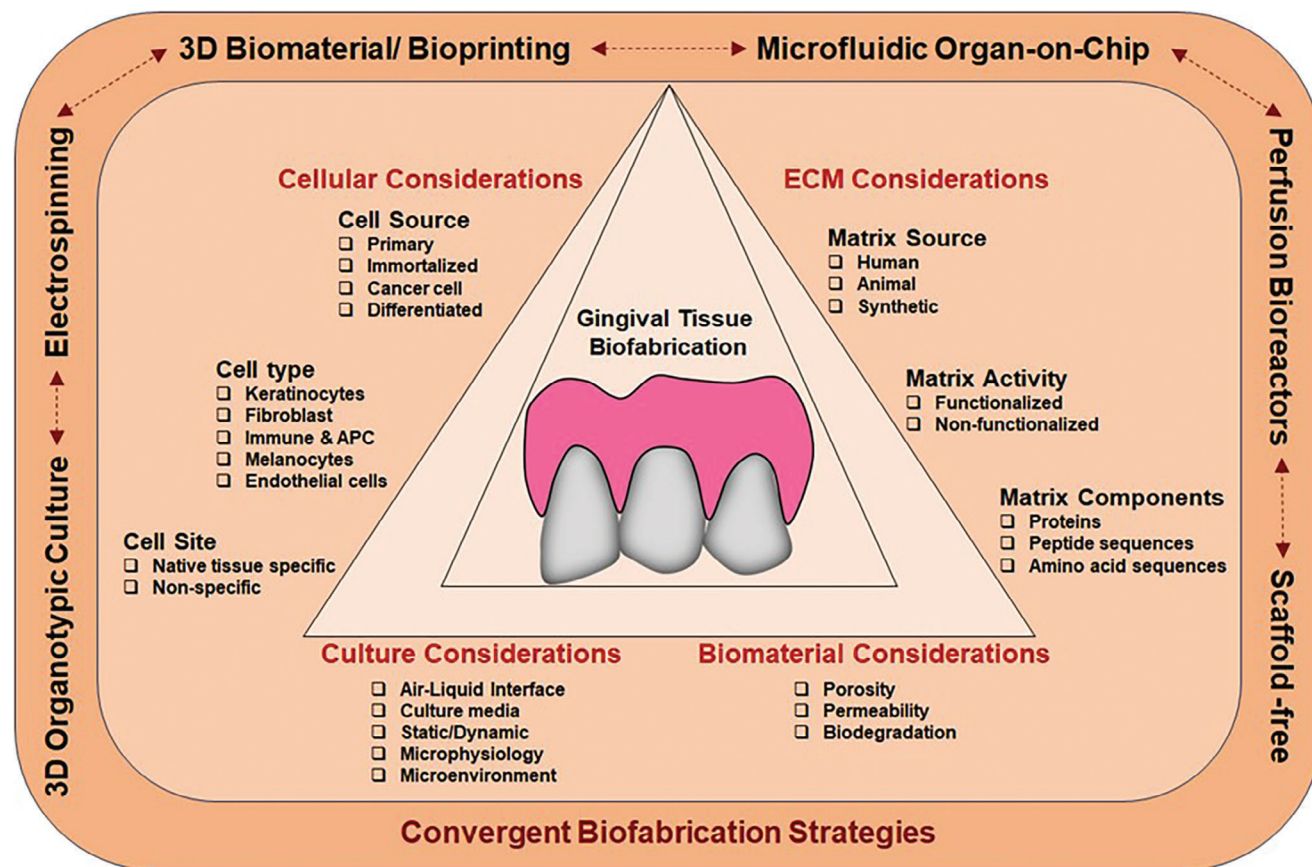


**Figure 3.** Schematic highlighting the key considerations and biofabrication strategies for fabricating next-generation gingival constructs.

optimal strategies for achieving requisite porosity. These multifaceted approaches enrich our understanding and pave the way for more effective design strategies in biomaterial development. The potential to precisely control pore size and distribution at various scales using 3D printing allows for replicating the natural hierarchy in gingival tissues, ensuring that the fabricated biomaterial or ECM closely mimics the native tissue's structural properties.<sup>[53]</sup>

### 3.1.2. Mechanical Properties

Mechanical considerations are paramount in biofabrication gingival tissue constructs, particularly given the substantial mechanical stresses that gingival tissues experience under masticatory load. Tensile strength, stiffness, and elasticity are crucial mechanical qualities that demand thorough evaluation to mimic the native tissue environment effectively. These attributes are pivotal to providing mechanical support for cell attachment, proliferation, and overall functionality. The essential mechanical properties requisite for bioengineering oral soft tissues, including the gingiva,<sup>[45]</sup> are shown in Figure 4B. Moreover, the mechanical properties ensure structural integrity during the handling and implantation. The tissue construct or scaffold must possess strong mechanical and structural properties that shield it from damage caused by the substantial forces of tissue tension or

occlusion. This resilience prevents unintended detachment and wound dehiscence.<sup>[41]</sup> Furthermore, the mechanical characteristics of the tissue-engineered scaffolds are critical in protecting the blood clot and promoting the healing process.

While synthetic biomaterials have excellent mechanical strength and tunability potential, their slow degradation is a limiting factor. In contrast, natural biomaterials like collagen, fibrin, and Fibro-Gide (bovine-collagen-based) have excellent biocompatibility and biological activity but poor mechanical properties.<sup>[54]</sup> Hence, hybrid biomaterials that combine synthetic material with tunable mechanical properties and natural polymers' biological activity have been widely studied.<sup>[55–56]</sup>

The three commonly used techniques for analyzing mechanical properties—monotonic uniaxial unconfined compression, small amplitude oscillatory shear (SAOS) rheology, and dynamic mechanical analysis (DMA)—offer different advantages and limitations. In gingival tissue analysis, DMA, particularly creep and small amplitude dynamic strain-controlled tests, are suggested for comprehensive mechanical characterization. SAOS rheology may be more suitable for studying processing kinetics due to its capacity to maintain volume integrity, which could be pertinent in assessing gingival tissue responses.<sup>[45]</sup> The mechanical properties of natural gingival tissue vary between individuals, influenced by age and sex. Nevertheless, through studies and analyses conducted on natural gingiva tissue under specific conditions—such as preconditioning with tensile forces ranging from 0.5 to

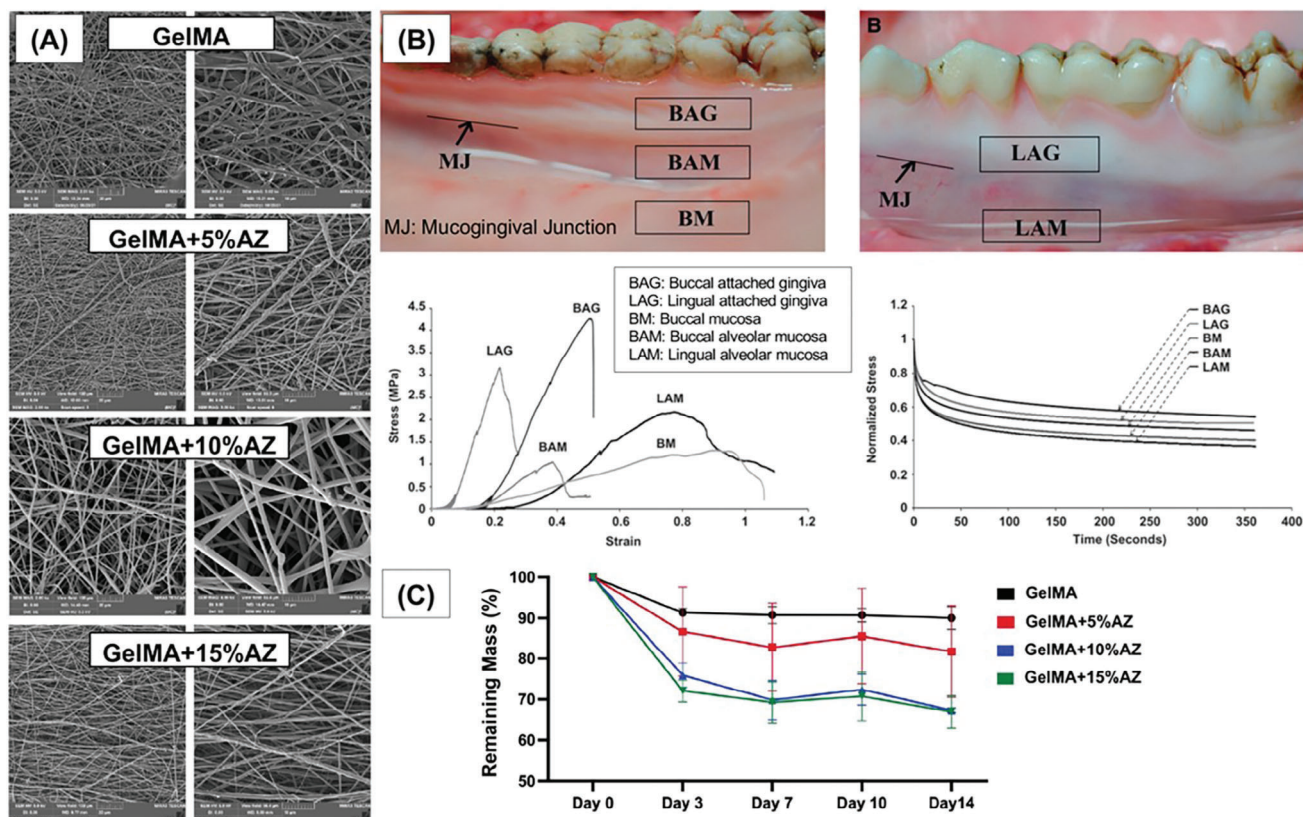


**Figure 4.** Characteristics and biodegradation profiles of electrospun gelatin-based fibers as scaffolds for oral soft tissue regeneration A) Scanning electron microscopy (SEM) images illustrating the fabrication of porous structures with permeability in electrospun gelatin-based fibers and pure GelMA fibers, as adapted from<sup>[44]</sup> open access article distributed under the terms and conditions of the Creative Commons Attribution (CC BY) license. B) Depictions of porcine oral soft tissues captured from the buccal and lingual perspectives of porcine lower jaws, stress-strain curves reflecting various regions of porcine oral mucosal tissue under uniaxial tensile testing, and a normalized stress relaxation curve, as adapted from,<sup>[45]</sup> Copyright 2021, John Wiley and Sons. C) Biodegradation profiles of different gelatin-based membranes over 14-day periods, adapted from,<sup>[44]</sup> an open-access article distributed under the terms and conditions of the Creative Commons Attribution (CC BY) license.

2.0 N over 20 cycles of stress/strain analysis at a rate of 20 mm min<sup>-1</sup> and utilizing specimens from Thiel-embalmed cadavers at 22 °C—the following mechanical characteristics were determined: natural gingival tissue exhibits a tensile strength of  $\approx 3.8$  MPa and an elastic modulus of  $\approx 37.4$  MPa.<sup>[57]</sup> Under conditions of compressive creep at 0.36 kPa, conducted at 37 °C for 5 min with a frequency of 1Hz, investigations were carried out on both hydrated and dehydrated mucosa. The results indicated that the elastic modulus of hydrated mucosa was  $\approx 2.7$  Pa, while that of dehydrated mucosa ranged from  $\approx 2$  to 4.5 Pa.<sup>[58]</sup>

The current standard of care for managing gingival recession commonly involves grafts from the hard palate, which exhibits a tensile strength of  $1.70 \pm 0.87$  MPa and an elastic modulus of  $18.1 \pm 4.5$  MPa.<sup>[57]</sup> The donor site selected is primarily the palate, as it offers connective tissue grafts that are suitable in thickness to match the needs of the recipient area. Nonetheless, aesthetic outcomes may be affected due to the color disparity between the graft and the tissues at the recipient site. Additionally, this approach presents the challenge of managing a significant denuded area in the palate, which requires healing through secondary intention.<sup>[59–60]</sup> Meanwhile, buccal mucosa, another candidate for autologous grafting to treat gingival reces-

sion, displays notably lower tensile strength ( $1.54 \pm 0.52$  MPa) and elastic modulus ( $8.3 \pm 5.8$  MPa) than graft from hard palate and gingiva (Figure 4B).<sup>[57]</sup> When designing gingival tissue, it is crucial to consider the mechanical stresses the engineered tissue will encounter, such as those generated by chewing, orthodontic movement, and wound healing dynamics, including blood flow and suture placements.<sup>[61]</sup> Researchers have emphasized assessing alternatives for oral soft tissue transplantation to examine cell-seeded biomaterials under physiological conditions. This exploration involves using bioreactors to simulate relevant conditions, such as imposition and control of shear stress on the cell-cultured biomaterial, allowing for an in-depth investigation into how these biomaterials and gingival constructs respond to critical factors.<sup>[61]</sup> Although this has promise as a screening technique for modified gingival tissue constructs, comprehensive in vivo data on forces experienced by the gingival tissues remains limited.<sup>[61]</sup> Additionally, the suture pull-out is another crucial mechanical attribute to be considered to ensure the grafts can withstand the shear forces exerted during suturing. The benchmark threshold for the pull-out test is at least 2N.<sup>[62]</sup>

Upon grafting, despite the biomechanical considerations, the findings demonstrated a significant decrease in keratinocytes

on skin-derived substrates (DED and AlloDerm) within the first week after implantation.<sup>[63]</sup> Moreover, epithelial cells from the autologous biopsy were also noted to diminish during this period. Observations indicated a decline in epithelial cells and deterioration of the graft. Intriguingly, when free gingival grafts were placed directly onto the bone, epithelial coverage was only restored after 14 days, primarily through growth from the wound edges. On the contrary, Yoshizawa et al. showed that the grafted ex vivo-produced oral mucosa equivalent (EVPOME) maintained its layered epithelial structure for up to 5 days postgrafting.<sup>[64]</sup> These results highlight the intricacies and variations in healing outcomes linked with different substrates, even when they possess appropriate mechanical characteristics.<sup>[65]</sup> In another study, engineered mucosal cell sheets resembling oral mucosa exhibited high flexibility and ease of handling.<sup>[66]</sup> In a rat model replicating tongue cancer surgery, these sheets facilitated oral wound healing by promoting re-epithelialization. They led to accelerated wound healing with minimal fibrosis, improving hand dexterity. The grafts also reduced inflammation and granulation formation, fostering a more natural healing process with enhanced hand functionality. These outcomes are possibly linked to improved microvascular formation and reduced fibrosis within the wounds.

### 3.1.3. Permeability

Lately linked to porosity, permeability is vital for efficiently transporting oxygen, nutrients, and signaling molecules within scaffolds, directly impacting cell viability and function. It is a crucial aspect of tissue engineering, requiring customization to meet the unique requirements of each engineered tissue and its operational environment. An optimal scaffold should facilitate the effective diffusion of essential nutrients and oxygen, alongside waste removal, to promote cellular health and proliferation. Furthermore, the scaffold's permeability should be designed to enable the infiltration of cells and the integration of the scaffold with the surrounding tissue without compromising the mechanical stability of the engineered construct.<sup>[23]</sup>

Achieving the ideal permeability level is a complex process influenced by the targeted biological objectives. For instance, studies have indicated that higher permeability can enhance bone formation in vivo, while lower permeability may improve cell seeding efficiency. Research conducted by Lien et al. found that chondrocytes exhibited increased proliferation and ECM production when cultured in scaffolds with pore sizes ranging from 250 to 500  $\mu\text{m}$ .<sup>[67]</sup> This range preserved cell phenotype, whereas smaller pores (50–200  $\mu\text{m}$ ) led to cell dedifferentiation.<sup>[67]</sup> Further studies on synthetic human elastin (SHE) scaffolds have shown that those with a 34.4% porosity and an 11- $\mu\text{m}$  average pore size effectively promote dermal fibroblast infiltration.

In contrast, scaffolds featuring a 14.5% porosity and 8- $\mu\text{m}$  average pore size were more conducive to surface-level cell proliferation.<sup>[68]</sup> Additionally, fibroblasts cultured in the scaffolds with higher porosity and larger pore sizes were observed to produce substantial quantities of fibronectin and collagen type I throughout the study, indicating a positive impact on extracellular matrix composition and scaffold integration.<sup>[68]</sup>

The ideal pore size for maximizing osteoblast activity within tissue-engineered scaffolds for bone regeneration remains to be determined, with studies presenting varying results. Scaffolds in bone tissue engineering typically feature pore sizes ranging from 20 to 1500  $\mu\text{m}$ .<sup>[69–72]</sup> Research by Akay et al. on osteoblast behavior in PolyHIPE polymer (PHP), a highly porous polymeric foam, revealed that osteoblasts tended to populate denser in areas with smaller pores (around 40  $\mu\text{m}$ ). In contrast, larger pores ( $\approx$ 100  $\mu\text{m}$ ) were more conducive to cell migration.<sup>[73]</sup> However, other findings disagree, showing that pore sizes larger than 300  $\mu\text{m}$  are necessary to facilitate osteogenesis.<sup>[74]</sup> Angiogenesis-wise, it is noted that a minimum porosity of  $\approx$ 30–40  $\mu\text{m}$  is essential for blood vessel regeneration, as it allows for the effective exchange of metabolic components and facilitates the entry of endothelial cells, ensuring a conducive environment for tissue development and integration.<sup>[41,75–76]</sup>

The physical attribute of mass transport represents the impact of structural design features on fluid flow dynamics within a construct. Porosity, pore structure, and permeability are three interrelated architectural features that impact the scaffold's diffusion dynamics and mechanical characteristics.<sup>[77]</sup> For instance, the porosity and permeability of fibrin and collagen hydrogels assessed within a microfluidic device demonstrated lower porosity and permeability than collagen hydrogels.<sup>[78]</sup> Further, the porosity and permeability of fibrin hydrogels depend on the concentration of fibrinogen and thrombin used for the hydrogel fabrication.<sup>[79]</sup>

Macromolecular permeation and interstitial flow within the gingival connective tissue contribute to the gingival crevicular fluid's (GCF) flow dynamics and composition.<sup>[80]</sup> The GCF exhibits transudate and inflammatory exudate features with the flow rate and macromolecular composition dependent on the health or inflamed status of the gingival crevicular wall.<sup>[80]</sup> To understand the permeation characteristics of macromolecules through gingival connective tissue constructs reconstructed within a microfluidic gingival crevice-on-chip, Makkar et al.,<sup>[81]</sup> adopted simulation studies using computational fluid dynamics followed by validation using fluorescence recovery after photobleaching (FRAP)-based assay. The kinetics of diffusion (recovery half-time) of fluorescein-conjugated dextran macromolecules of 10 and 70 kDa sizes through photobleached area of the tissue constructs provided insights into the macromolecular perfusion characteristics representative of transudate and exudate, respectively.

### 3.1.4. Biodegradation

Ideally, the graft material's degradation rate should match the time required for gingival tissue regeneration. The degradation rate of a prospective replacement graft should be rapid enough to integrate the host and cultured cells successfully. However, it is also imperative that the graft retains its structural integrity and mechanical properties to ensure overall construct stability. Establishing a single, universally applicable design for gingival tissue engineering that effectively manages biodegradation presents significant challenges due to various influencing factors. The complexity of selecting the appropriate materials is central to these challenges, as this choice directly impacts the scaffold's



biodegradation rate, which must be carefully synchronized with the formation of new tissue. While the ideal graft is designed to both prevent the ingrowth of gingival epithelium into the defect and promote the recruitment and adhesion of native undifferentiated cells for new ligament tissue formation, achieving this balance is complicated by the need for a nuanced understanding of the healing process, expected to span 4 to 6 weeks for periodontal connective tissue. The scaffold's degradation should proceed at a pace that maintains its structural integrity throughout the regeneration period, aiding in the recruitment, proliferation, and differentiation of periodontal progenitor cells while simultaneously inhibiting the invasion of gingival epithelial cells into the defect area. This intricate interplay of requirements underscores the difficulty of developing a singular tissue engineering strategy to accommodate periodontal tissue regeneration's diverse and dynamic nature, influenced by patient-specific responses, material properties, and the scaffold's architectural features.

Ayoub and colleagues developed biodegradable azithromycin (AZ)-loaded gelatin methacryloyl (GelMA) electrospun fibers with controllable drug release for infection ablations (Figure 4C).<sup>[44]</sup> Previous work in a canine model assessed the therapeutic use and efficacy of ePTFE (Gore) and PLA (Guidor) membranes.<sup>[82]</sup> Generally, the nonresorbable ePTFE material is removed between 4 and 6 weeks after implantation. Therefore, nonbiodegradable materials are not designed for cellular infiltration, which is necessary for forming functional gingival tissue during gingival regeneration. There is plenty of evidence in the literature to show that the underlying connective tissue supports and controls epithelial development and cellular differentiation.<sup>[83]</sup> For example, if an implanted material were to deteriorate too fast (in less than 16 weeks), volume loss and inadequate or nonexistent tissue growth would result. There is no evidence of tissue infiltration or functional tissue regeneration, such as cellular interactions with the vascular network of the basement membrane when long-lasting grafts like Artelon or PTFE-polyvinylidene fluoride-polypropylene (PP) tetrapolymer are used.<sup>[84]</sup> Degradation studies of the Geistlich Fibro-Gide product show that tissue remodeling and healing continue 3 months after implantation, with blood vessels forming in the graft.<sup>[85]</sup> Degraded Fibro-Gide graft usually loses its physical structure rapidly, adversely influencing graft efficiency.<sup>[86]</sup>

### 3.2. Cellular and Biological Considerations

Fabricating gum tissues *in vitro* requires the incorporation of cellular and biomechanical cues, which promote the spatial organization of the gingival keratinocytes to form a stratified, multilayered epithelium with cornification. A significant factor in achieving keratinocyte's desired stratification and differentiation involves exposing the biofabricated construct to an air-liquid interface (ALI). This positioning allows the construct's apical end (keratinocyte seeded side) to be exposed to air while the basal side experiences the diffusion of culture media.<sup>[87–89]</sup> Culture at ALI and under high calcium levels induces polarization of the basal keratinocyte shift in the cell division axis, leading to stratification and differentiation. Another crucial cue is provided by the gingival fibroblasts, which engage in crosstalk with overlying keratinocytes and secrete soluble factors, such

as growth factors and cytokines. These molecular signals play a crucial role in orchestrating the spatiotemporal aspects of epithelial morphogenesis.<sup>[89–92]</sup> These biological principles have inspired the development of organotypic gingival tissue models, ranging from reconstructed gingival epithelium-only models to full-thickness gingival equivalents.<sup>[13,93]</sup> Reconstructed gingival epithelium-only models are relatively simplistic and fabricated by seeding oral or gingival keratinocytes over an acellular porous membrane or collagen scaffold within a Transwell, followed by ALI culture to induce stratification and differentiation.<sup>[94]</sup> In contrast, full-thickness models involve seeding the keratinocytes over a fibroblast-laden matrix, typically collagen and fibrin-based hydrogels, followed by ALI culture.<sup>[16,87–88,95–97]</sup>

#### 3.2.1. Cellular Considerations

In regenerative medicine, many cells are employed to repair, replace, regenerate, and improve the function of tissues or organs. These cells include embryonic stem cells (ESCs), which have the potential to differentiate into any cell type; adult stem cells, such as mesenchymal stem cells (MSCs) found in bone marrow, adipose tissue, and dental pulp, known for their ability to differentiate into a variety of tissue types including bone, cartilage, and fat; and induced pluripotent stem cells (iPSCs), which are adult cells reprogrammed into an embryonic stem cell-like state, capable of differentiating into many different cell types. Within the intricate structure of gingival tissues, a diverse array of cell types collectively contributes to their multifaceted nature. The cell types most commonly utilized include periodontal ligament stem cells (PDLSCs), gingival mesenchymal stem cells (GMSCs), and bone marrow-derived mesenchymal stem cells (BMSCs). These cells are particularly valued for their capacity to promote the regeneration of periodontal tissues, including the gingiva, periodontal ligament, and alveolar bone. PDLSCs are especially crucial for their role in regenerating the periodontal ligament and supporting structures of the teeth. GMSCs, harvested from the gingiva, are advantageous due to their accessibility, proliferative capacity, and potential to differentiate into multiple cell types, contributing significantly to the repair and regeneration of gingival tissue. These cells facilitate the structural repair of damaged tissues and secrete bioactive factors that modulate the immune response and enhance healing, making them pivotal in developing effective strategies for gingival regeneration in regenerative dentistry.<sup>[98–100]</sup>

In the gingival epithelium, keratinocytes are the predominant cell type.<sup>[101]</sup> The gingival keratinocytes form a keratinized stratified squamous epithelium consisting of basal, spinous, granular, and corneal layers.<sup>[101]</sup> The gingival epithelium contains other cell types, such as Langerhans, Merkel, and melanocytes.<sup>[101]</sup> Complementing the complexity, the gingival connective tissue (also termed lamina propria) presents two distinct layers: the reticular layer proximal to the tooth-root surface or the alveolar bone and the papillary layer that is intertwined with the rete pegs of the gingival epithelium.<sup>[101]</sup> The lamina propria comprises cells, ECM, blood vessels, lymphatic vessels, and nerves.<sup>[101]</sup> This environment is further enriched by additional cell types that include neutrophils, resident macrophages, mast cells, and those involved in inflammation and innate immune response.<sup>[101]</sup> This

intricate cellular interplay orchestrates the complex architecture and functional dynamics of gingival tissues.

In this way, one of the crucial considerations for the biofabrication of gingival tissues is the selection of relevant cells and their sources.<sup>[102]</sup> This is significant when recapitulating native tissue's barrier and host defense properties, which are crucial.<sup>[103]</sup> The various cell types used to biofabricate gingival tissue constructs range from primary, immortalized, and tumor-derived cell lines.<sup>[102]</sup> Among these options, primary cells hold a significant advantage due to their close phenotypic resemblance to cells found in vivo.<sup>[104]</sup> However, a considerable challenge in primary cell use includes post-mitotic alterations and senescence under in vitro culture and expansion.<sup>[105]</sup> This limits their use in laboratory settings, especially when large quantities of cells are required for tissue engineering and regenerative applications. Furthermore, factors such as donor age, tissue origin, health/disease status, and the distinction between single versus pooled donors can collectively influence the variability in outcomes concerning cell performance and bioactivity of the cells for gingival tissue engineering.

Cancer cells and immortalized cell lines have an immense potential to be alternatives to primary cells in the early phases of developing gingival tissue models. They have been used extensively to reconstruct gingival tissue equivalents for investigating mucosal barrier properties, host-microbe, and host-material interactions.<sup>[14]</sup> Human oral cancer cell lines TR146 and HO-1-u-1 have commonly been used for permeation-based studies.<sup>[106–108]</sup> They are derived from metastatic buccal carcinoma and squamous cell carcinoma of the floor of the mouth, respectively.<sup>[93]</sup> However, these cells have questionable physiological relevance and are shown to form loose epithelium without tight junction proteins.<sup>[107,109]</sup> Alternatively, immortalized gingival keratinocytes and fibroblasts have gained popularity in developing full-thickness gum tissues. Immortalization of oral cells can be performed by various methods, which include silencing of tumor suppressor gene p53, using viral oncogenes like HPV E6/7, or by telomerase reverse transcriptase expression (TERT).<sup>[110]</sup> Unlike other immortalized keratinocytes, TERT-immortalized keratinocytes can combine the physiological attributes of primary cells and the long in vitro culture span.<sup>[89,111]</sup> These cells exhibit stable karyotypes and can be induced to become differentiated cells showing tissue-specific features and expressing differentiation-specific proteins.<sup>[112–113]</sup> Past attempts to use TERT immortalized keratinocytes from the gingiva and floor of the mouth, as well as gingival fibroblasts, led to the development of organotypic culture of oral mucosa and gingiva for host material and microbe interaction studies.<sup>[16,95–96,111]</sup> Histological and immunohistochemistry data from these studies has shown the advantages of these cells to generate oral mucosa/gingiva equivalents in vitro with well-organized multilayered epithelium, culture time-dependent expression of key epithelial differentiation markers, cytokeratins, and antimicrobial peptides similar to the native tissue.<sup>[95,114]</sup>

Incorporating a cellular subepithelial layer in the full-thickness model facilitates epithelial–mesenchymal crosstalk, which aids in enhanced differentiation of epithelium that closely mimics the native gingival tissue. Another essential biological consideration should be given to the type of fibroblasts used in the biofabrication process. Fibroblasts maintain positional and topograph-

ical identity, determining their function.<sup>[89,92,115–116]</sup> In the context of gingival tissues, high heterogeneity among the gingival fibroblast population has been observed using single-cell sequencing techniques.<sup>[117]</sup> The fibroblasts in the superficial connective tissue (one just below the epithelium) are distinct from those present in the deeper gingival connective tissue, and past studies using 3D cultures have shown this dictating differences in epithelial morphogenesis and innate immune response.<sup>[90–92]</sup>

### 3.2.2. Extracellular Matrix Components

Collagens, elastin, laminin, and fibronectin are the main components of the connective tissue matrix of healthy gingiva.<sup>[118–120]</sup> Notably, collagen types I and III constitute the majority of collagen within the human gingival tissue.<sup>[118]</sup> Collagen type IV and V collagen constitute a mere 1%, predominantly present during the early recovery phases of wound healing. Collagen type V is suggested to direct endothelial cells (ECs), enhancing vascularization and angiogenesis.<sup>[118]</sup> In this intricate milieu of the lamina propria, human gingival fibroblasts (HGFs) play a pivotal role in ECM synthesis and maintenance.<sup>[121]</sup> Within every cubic millimeter of the lamina propria, a staggering population of  $\approx 200$  million fibroblasts exists.<sup>[122]</sup> This dynamic fibroblast network generates an assortment of constituents, including collagen fibers, that are organized to meet the mechanical demands of the gingival tissue. The collagen fibrils produced by HGFs typically range between 50 and 100 nm.<sup>[122]</sup>

In addition to incorporating different cell types, the interaction between biomaterials and cell types is crucial for de novo collagen, elastin, laminin, and fibronectin production and organization. Noninvasive imaging techniques, such as confocal reflectance microscopy and second harmonic generation microscopy, have provided valuable insights into the behavior of HGFs and periodontal ligament-derived fibroblasts when embedded within collagen-free human fibrin-based matrices.<sup>[81,88,92]</sup> These studies reveal the remarkable capacity of these cells to generate a de novo reticular network of ECM fibers characterized by a substantial presence of collagen and fibronectin. These cell-derived reticular ECM fibers are interspersed between the amorphous native fibrin matrix and organized around the vasculature.<sup>[123]</sup>

Furthermore, the fibroblasts exhibit age-associated qualitative alterations in the ECM fiber organization.<sup>[124]</sup> Young fibroblasts exhibit a robust ECM production, featuring a dense accumulation of collagen and fibronectin intricately woven into a complex reticular pattern. Conversely, aged fibroblasts generate a thinner ECM structure with a more linear alignment of its constituent fibers.<sup>[124]</sup> Further, it has been recently reported that the implantation of engineered gelatin-based nanofibers supported angiogenesis, the integration with host tissue, based on the presence of mature, thick, and well-aligned collagen fibers intertwining with the scaffold while promoting mild inflammatory response.<sup>[44]</sup>

### 3.2.3. Vascularization

Incorporating vasculature within gingival tissue constructs provides vital functionality with the prospects of enabling

rapid inosculation and integration with host vasculature, oxygenation, nutrient transport, removal of metabolic waste, and host innate and adaptive defense.<sup>[125]</sup> Tissue constructs with microvascular networks have been fabricated using 3D culture and self-assembly of endothelial and mural cells,<sup>[123,126–127]</sup> 3D bioprinting,<sup>[128–130]</sup> and microfluidic organ-on-chip systems.<sup>[131–132]</sup> Some key considerations for incorporating vasculature within the gingival constructs include the source of endothelial cells, ranging from microvascular origin or large vessels.<sup>[123,127,130,132–133]</sup> Additionally, incorporating mesenchymal stromal or mural cells is essential for vascular maturation and function.<sup>[127]</sup> The source of stromal cells and their ratio to endothelial cells can play a crucial role in angiogenic events, vascular maturation, and barrier function.<sup>[127,134–136]</sup>

Integrating blood vessels into tissue equivalents remains an ongoing challenge, demanding optimization of cell culture conditions, biomaterial selection, fabrication methodologies, and comprehensive clinical investigations.<sup>[138]</sup> Makkar et al.,<sup>[123]</sup> recently demonstrated the fabrication of vascularized gingival connective tissue equivalents using primary gingival fibroblasts and endothelial cells of microvascular origin embedded within a fibrin-based matrix (Figure 6A–C).

Further, they demonstrated the application of the model for understanding periodontal host-microbe interactions using coculture with an array of early, intermediate, and late biofilm colonizers (Figure 6D). Interestingly, the secretome from these vascularized tissue equivalents exposed to various bacterial colonizers exhibited differential polarization of macrophages towards pro-inflammatory and anti-inflammatory phenotypes.<sup>[123]</sup> Similarly, Gard et al. designed a high-throughput microfluidic model to investigate gingival tissue's inflammation and subsequent healing.<sup>[137]</sup> Through the visualization of human microvascular endothelial cells (hMVECs), they observed that a robust and well-preserved endothelial layer could be maintained throughout extended culture until day 32, as shown in Figure 5A–C.

Similarly, Nishiyama et al. employed a layer-by-layer cell coating technique to fabricate vascularized oral mucosa equivalents exhibiting keratinized and nonkeratinized phenotypes (Figure 6E).<sup>[139]</sup> However, control over microvessel diameter and distribution remained challenging. Similarly, Heller et al. demonstrated the fabrication of prevascularized buccal mucosa equivalents using a triculture of keratinocytes, endothelial cells, and fibroblasts on a collagen matrix (Bio-Gide).<sup>[140]</sup> Transplantation of these constructs into nude mice resulted in accelerated blood supply through functional anastomosis with host vasculature. Despite these advancements, capillary-like structures within the collagen matrix appeared nonuniform, primarily concentrated near the surface. The authors postulated that limited endothelial cell infiltration might arise from insufficient angiogenic factor signaling and/or matrix-related structural constraints.

Looking ahead, the integration of 3D bioprinting technology holds promise for developing gingival grafts featuring intricate hierarchical vasculature encompassing major and minor vessels. Achieving gingival tissues with complex vascular architecture necessitates a comprehensive understanding of the native tissue's vasculature and acquiring a vascular blueprint. However, inherent structural variations in gingival vasculature are apparent.<sup>[141]</sup>

The extent of the anastomosis of prevascularized constructs depends on the type and degree of blood flow directed toward the lamina propria.<sup>[142]</sup> Prior studies have shown heterogeneity in the vascular organization with more horizontal or vertical blood flow following selective occlusion of particular parts of the papilla.<sup>[141]</sup> This could be attributed to the dense network of blood vessels within the gingiva.<sup>[141]</sup> Arteriole-to-arteriole linkages may have a role in the observed discrepancies.<sup>[141,143]</sup> In the papillary component, terminal capillary loops intricately interconnect with post-capillary venules within the gingival plexus, creating a dense vascular network.<sup>[122]</sup> About 50–60 loops  $\text{mm}^{-2}$  are in the papillary layer.<sup>[122]</sup> Remarkably, the natural gingival tissue hosts up to 10 microvessels  $\text{mm}^{-2}$ , with the size of each vessel distinctly tailored to its specific anatomical location and hierarchical level.<sup>[144]</sup>

Furthermore, gender distinctions exist, with men exhibiting greater recovery of blood flow and rapid anastomosis of coronally advanced flaps compared to women.<sup>[145]</sup> This divergence might offer critical insights that could be harnessed to foster graft anastomosis. To effectively extend the application of prevascularization strategies to gingival tissue regeneration, it becomes imperative to characterize the nuances inherent in gingival vasculature. Considering gingival tissue's physiological and anatomical features, regulating blood vessel growth is vital for successful graft integration and effective healing.<sup>[142]</sup>

#### 4. Biofabrication Strategies

Gingival tissue engineering aims to restore the original design and function of the gingival structure, involving soft-to-hard tissue integration. Scaffold-based and scaffold-free biofabrication approaches have considerably evolved with the advancements in dental biomaterials and regenerative tissue engineering strategies.<sup>[146]</sup> Using cells, growth factors, bioactive agents, and biodegradable and mechanically durable polymeric scaffolds, scaffold-based strategies can retain cells and increase their survival rates in response to unique therapeutic demands.<sup>[146]</sup> Variations in architecture and geometry (porosity, pore structure, etc.) and chemical composition characterize a multiphase (e.g., varying materials, chemical/morphological structures, and mechanical properties) scaffold, which often resembles normal gingival tissue in terms of its structural arrangement or cellular and molecular makeup.<sup>[147]</sup> Multiphase scaffolds, which may provide tissue-engineered bone and soft tissue grafts with biomimetic activity, have recently been used in dental tissue engineering. Soft-hard tissue interface control is often required during gingival tissue restoration.<sup>[148]</sup>

Furthermore, similar to gingiva regeneration, the failure to accomplish functional integration of heterogeneous soft and hard tissue, either with one another or with the host environment, represents a substantial therapeutic gap. Sometimes, the original soft and hard tissue architecture may be restored by adopting a sophisticated scaffold design, allowing for effective tissue integration *in vivo*.<sup>[146]</sup> Biofabrication technologies, including fused deposition modeling, electrospinning, 3D printing, and bioprinting, have regenerated a multiphase structure.<sup>[149]</sup> Alternatively, prefabricated multicellular building blocks such as spheroids, cell sheets, exosomes, and tissue strands are studied through scaffold-free tissue engineering.<sup>[146,150]</sup> The modular bottom-up approach replicates the microenvironment of the

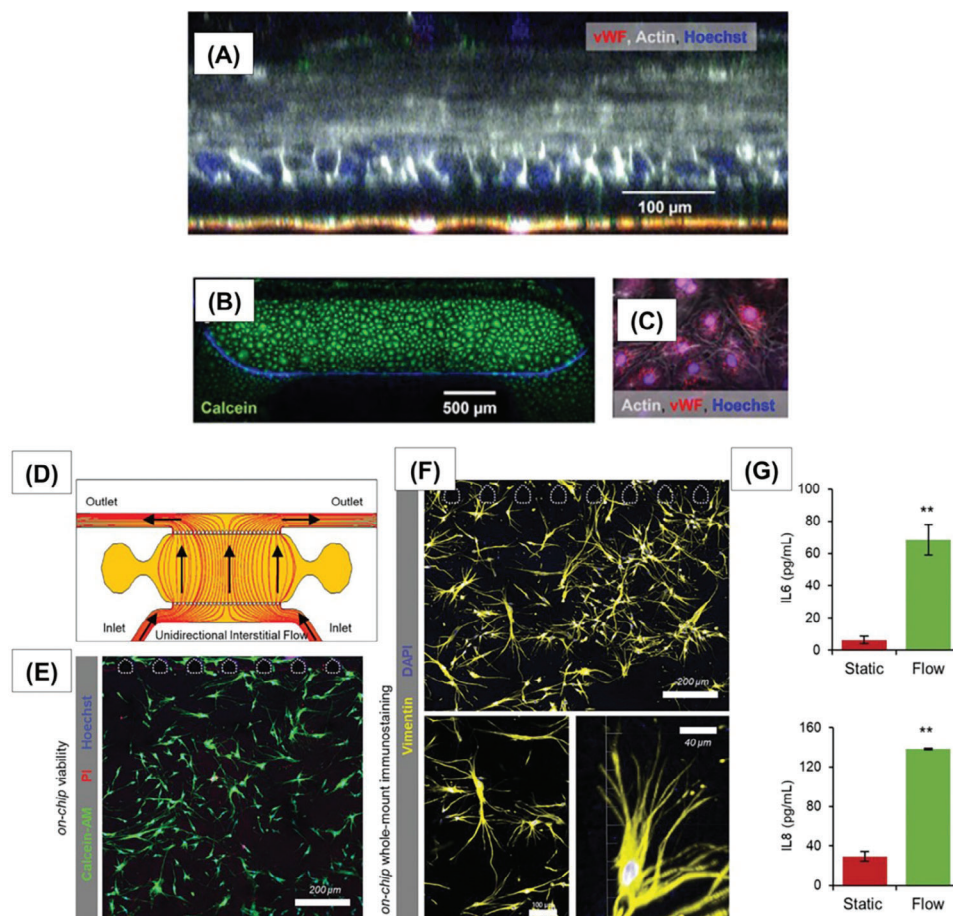


**Figure 5.** Culturing gingival constructs under flow using organ-on-chip system and its impact on cellular morphology and function. A) Confocal orthogonal view of the engineered tissue. B) Observation of a layer of human microvascular ECs on day 32. C) Specific staining of the vascular-related marker von Willebrand factor (in red) indicates blood vessels on the lower side of the membrane. Reprinted from.<sup>[137]</sup> Distributed under the terms of the Creative Commons Attribution License (CC BY). D) Schematic representation illustrating the gingival compartment exposed to unidirectional interstitial flow. E) Evaluation of cell viability in gingival fibroblasts after a 9-day culture on a microfluidic chip, influenced by interstitial flow. F) Visualization of vimentin-positive fibroblasts within the fibrin matrix, displaying a spindle-shaped morphology with numerous slender and elongated dendritic extensions. G) Examination of the secretome in media collected from the outlet ports, highlighting the impact of interstitial flow on the increased constitutive secretion of IL-6 and IL-8, which play a role in maintaining periodontal homeostasis. D–G) Adapted from,<sup>[81]</sup> Copyright 2021, John Wiley and Sons.

tissue by allowing monodispersed cells to self-assemble into 3D tissue with cell-cell and cell-matrix interactions.

#### 4.1. Electrospinning

Electrospinning is a potentially valuable bioengineering technology for gingival tissue regeneration. This technique allows for the generation of fibers and fibril characteristics similar to those of the host extracellular matrix (ECM). For example, electrospinning enables the creation of diverse pore sizes through precise control of fiber diameter.<sup>[44]</sup> Electrospinning can form fibers with diameters similar to collagen and other necessary supporting fibers like elastin. Fibrillar collagen types I and II have a diameter between 25 and 400 nm.<sup>[151–152]</sup> Fibrillar elastin has a diameter of 0.2 μm, whereas a single elastin fiber is around 1 μm in diameter.<sup>[153]</sup> These ultimately fall within the range of fiber diameters achievable using electrospinning.<sup>[154]</sup> The underlying rele-

vance and importance of having fiber diameters recapitulating those found in natural tissue are complicated and likely dependent on whether the graft is meant to be preseeded with cells or be employed as an acellular graft. Human umbilical vein endothelial cells (HUVECs) had considerably higher scaffold infiltration, vitality, and CD31 expression when the fiber diameter was 4.83 μm compared to fiber diameters ranging from 1.64 to 3.37 μm.<sup>[155]</sup>

Similarly, Ramezani et al. investigated the function of human umbilical vein endothelial cells (HUVEC) seeded on different electrospun scaffolds over 24 h, followed by implantation on mouse skin for 4 weeks. Histological analysis revealed distinct layers, including the epidermis, dermis, scaffold, and microvessels, as shown in **Figure 7A,B**.<sup>[156]</sup> In another work, researchers cultured vascular smooth muscle cells (VSMC) onto PCL fibers with different fiber diameters. They found that fiber diameter scaffolds of 7 and 10 μm permitted higher VSMC and macrophage infiltration than lower fiber diameter scaffolds.<sup>[157]</sup> Despite the availability of various porosities and fiber diameters

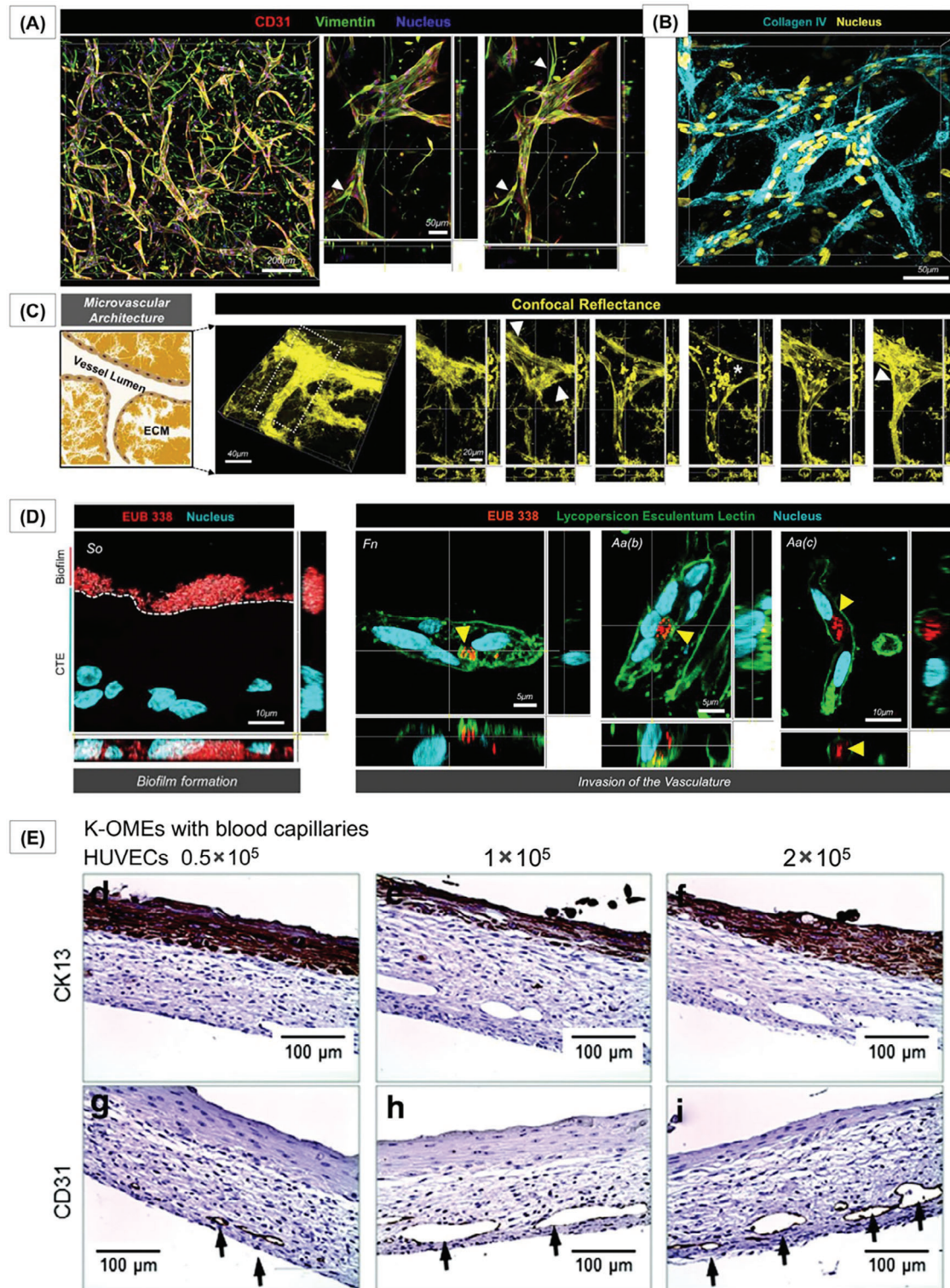


**Figure 6.** Vascularized gingival constructs. Confocal z-projection micrographs of whole-mount immunostained vascularized gingival connective tissue equivalents (CTEs) showing A) CD31, vimentin-positive, and B) Collagen IV positive microvessels that exhibit tortuous morphology, extensive branching, and anastomosis across the fibrin matrix. C) Label-free confocal reflectance microscopic of vascularized gingival CTEs showing microvascular architecture with polarized endothelial cells that encircle the patent vessel lumen. D) Confocal images of tissue sections hybridized with pan-bacteria FISH probe EUB 338 showing well-defined biofilm formation by early *S. oralis* and microvascular invasion (yellow arrowheads) by *F. nucleatum* and *Aggregatibacter actinomycetemcomitans*. A–D) Adapted from reference,<sup>[123]</sup> Copyright, IOP Publishing. E) Immunostained (CK13 and CD31) images of vascularized oral mucosal equivalents fabricated using varying densities of endothelial cells demonstrate the presence of CD31-positive microvessels. E) Adapted from reference,<sup>[139]</sup> Copyright 2019, Mary Ann Liebert, Inc.

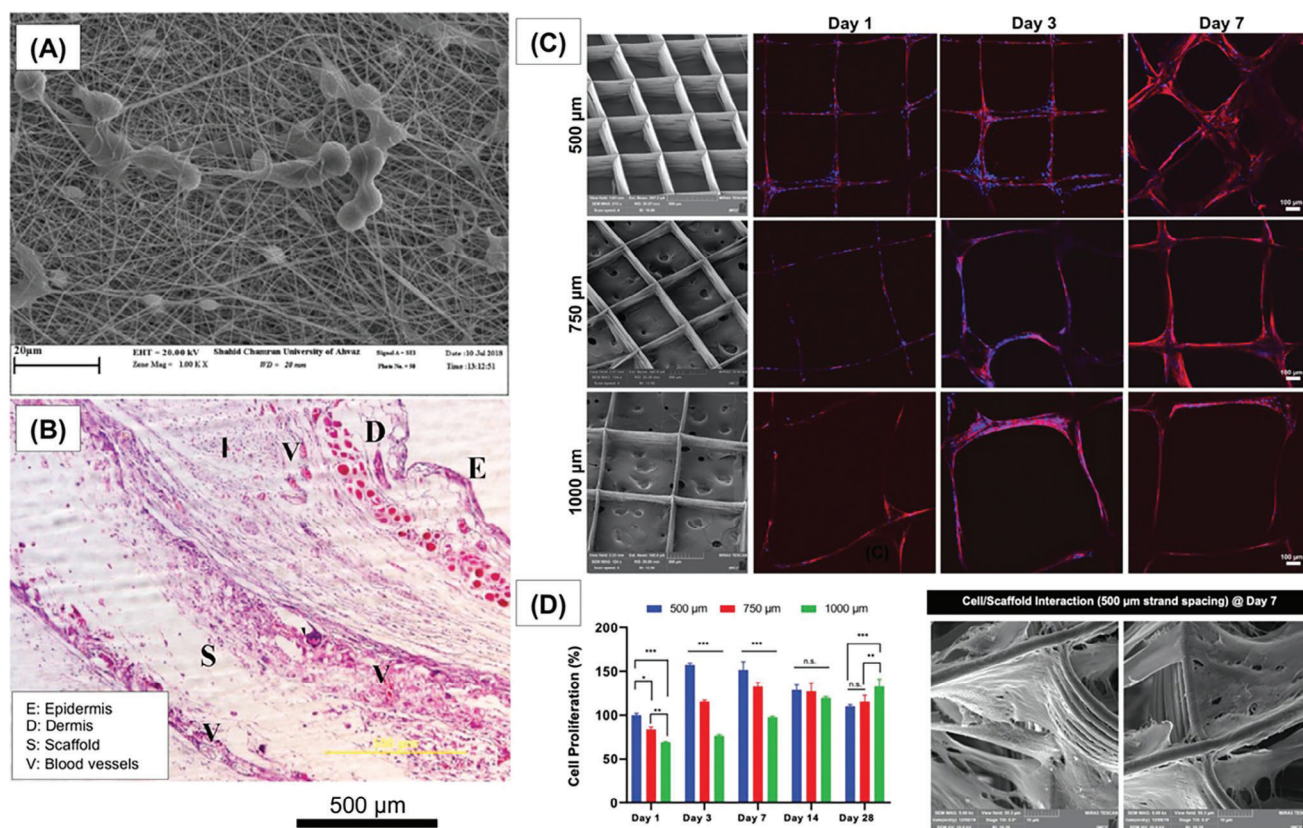


**Figure 7.** Nanostructures and nanofibrous scaffolds for oral soft tissue engineering applications. A) Scanning electron micrographs display the cell morphology of human umbilical vein endothelial cells (HUVEC) when cultured on different electrospun scaffolds for 24 hours. B) An image from histology shows a four-week integration of an electrospun scaffold into mouse skin, illustrating distinct layers. Adapted from,<sup>[156]</sup> Copyright 2021, Elsevier Inc.; C) Shown here are representative scanning electron microscopy (SEM) images of PCL scaffolds fabricated using Melt ElectroWriting (MEW) technology featuring various strand spacing. Additionally, confocal microscopy images capture human periodontal ligament stem cells (hPDLSCs) cultivated on these scaffolds for 7 days (fluorescent staining using DAPI (in blue) and phalloidin (in red)). The scale bar is set at 100 μm. D) The proliferation of hPDLSCs and SEM images depicting their growth on MEW PCL scaffolds over 28 days are quantified. These findings are adapted from,<sup>[158]</sup> Copyright 2021, John Wiley and Sons.

that alter cellular phenotype in the literature, there seems to be no established standard for gingival tissue engineering.

Electrospun scaffolds may be engineered to be highly similar to the native ECM. However, a single-layer electrospun membrane does not allow for the fabrication of tissues with significant thicknesses and heterogeneous cellular densities.<sup>[159]</sup> Therefore, there has been a rise in the use of multilayer electrospun scaffolds.<sup>[160]</sup> Gingival tissue has transverse and longitudinal layers. The free gingiva has vertically stacked layers of squamous epithelial tissue supported by a dense connective tissue matrix, whereas the connected gingiva has a honeycomb structure.<sup>[160]</sup> Abedi et al. demonstrated multilayer electrospun scaffolds resembling gingival tissue structurally replicating the natural gingiva. There are three major layers of horizontally oriented gingival tissue: the epithelium, which is composed of many layers of keratinocytes with various and intricate functionalities,<sup>[160]</sup> lamina propria (a papillary and reticular layer containing gingival fibroblasts, vasculature, and collagen-rich ECM) and the basement membrane.<sup>[161]</sup> After just one week, blood cells were found in the middle of a three-layer structure, demonstrating that stacking electrospun scaffolds (polycaprolactone and polycapro-

lactone/collagen) cultured with either endothelial cells or fibroblasts accelerated the development of capillaries in an *in vivo* rat model.<sup>[162]</sup> Vasculature development was shown to rely on the presence of endothelial cells and the thickness of the electrospun scaffold. This provides evidence that multilayer electrospun scaffolds may promote vasculature development in a manner expected to allow the transport of waste products, oxygen, and nutrients, hence promoting tissue regeneration. One week after implantation *in vivo*, a three-layered construct harboring red blood cells was observed. Electrospun multilayered structures cultured with fibroblasts and endothelial cells offer a sufficient environment for vessel development.<sup>[162]</sup> Given the presence of vasculature in natural gingiva (10 lumens mm<sup>-2</sup>), multilayer electrospun scaffolds promote the creation of vasculature.<sup>[163]</sup> However, more clinically relevant animal models are required to analyze these multilayered scaffolds regarding their potential for gingival tissue regeneration.

Larger pores were hypothesized to assist in the fusion of the gingiva with the new alveolar bone. The membrane used to build the structure has macroscopic pores; high flexibility and resilience are needed to support the cell sheet. In an ectopic

periodontal regeneration model in athymic rats, the biphasic architecture combined with the cell sheet approach enabled the development of osteoblasts in the bone compartment before subcutaneous implantation. In the presence of the cell sheets, a ligament-like tissue developed, which enhanced the attachment onto dentin and was well integrated into the generated bone.<sup>[164]</sup> Scaffolds made by 3D melt electrospinning have the permeability and “sponge-like” consistency needed to better conform to gingival defects’ irregular shapes and sizes. In this regard, 3D electrospun polycaprolactone (PCL) scaffolds cocultured with osteoblasts have been found to stimulate the formation of bone in an ectopic rat model.<sup>[165]</sup>

In addition to porosity, micron-sized laser-cut ablations have been previously developed using layers of an electrospun poly (lactic acid) scaffold, further enhancing the functionality of the multilayered electrospun platforms. Human adipose-derived stem cells (ASCs) were presented to proliferate and survive better in the laser-cut pores, around 300 µm in diameter,<sup>[157]</sup> compared with nonablated structures. Furthermore, the ablations prevented the scaffold layers’ separation and kept the multilayered structure intact.<sup>[166]</sup> Before layering, collagen type I was pipetted onto the fibers to strengthen the bond between the scaffold layers and to incorporate biological motifs to enhance biological activity. Laser-cut ablations may provide a strategy to reduce electrospun scaffold layer separation and promote cell survival and proliferation.<sup>[166]</sup>

#### 4.2. 3D Biomaterial Printing

3D printing is a technology that creates three-dimensional objects using computer-aided design (CAD) software and specific materials. The field of dentistry, and periodontics, in particular, has significantly benefited from 3D printing technology. The regeneration of periodontal tissues, including alveolar bone, periodontal ligaments (PDL), and cementum, has been studied using 3D printing techniques.<sup>[53,167]</sup> This includes gingival lesions (treatment of gingival recessions, gingivectomies, or restoration of the smile design). Recently, Daghery et al. utilized Melt ElectroWriting (MEW) to engineer highly ordered scaffolds (Figure 7C–D).<sup>[158]</sup> They studied the adhesion, proliferation, and osteogenic differentiation of cultured human periodontal ligament stem cells (hPDLSCs) and the impact of strand distance and the addition of nanostructured fluorinated calcium phosphate (F/CaP) on tissue regeneration. Excellent periodontal regeneration was observed both in vitro and in vivo, suggesting the possibility of antimicrobial protection and simultaneous, synchronized restoration of both soft and hard periodontal tissues.<sup>[158]</sup>

To repair calvarial abnormalities in rabbits, Wang et al. created a bilayered scaffold model composed of collagen and strontium-doped calcium silicate containing gingival fibroblast cells.<sup>[168]</sup> Bilayered scaffolds were reported to enhance osteogenesis.<sup>[168]</sup> Using co-axial electrospinning and 3D printing, Dos Santos et al. developed zein-based bilayers that might be used as a dual-drug delivery platform.<sup>[169]</sup> Human oral keratinocytes (Nok-si) cell survival was over 80%, and antibacterial activity against bacterial strains (*Treponema denticola* and *Porphyromonas gingivalis*) was shown in vitro for the two-layer constructions that allowed the controlled delivery of various drugs over 8 days.<sup>[169]</sup>

Controlling fiber orientation and aiding the formation of the periodontal tissue complex was the focus of another multiphased method.<sup>[170]</sup> This method relied on computational scaffold design and fabrication by 3D wax printing to implement a multicompartmental construct architecture. Cells transduced with a recombinant adenovirus expressing murine bone morphogenetic protein 7 (AdBMP-7) were cultured on PCL-polyglycolic acid scaffolds. Newly manufactured tissues in an in vivo study in nude mice showed the interfacial development of parallel and obliquely aligned fibers, which generated human tooth dentin-ligament-bone tissue.<sup>[171]</sup> Bone and cementum were formed on dentin surfaces only in AdBMP-7-treated gingival cells but not in nontreated cells. Since adenovirus-transduced cells may be regulated, this technique may have translational limitations. The perpendicularly oriented microchannels created by the 3D wax/solvent casting process were then examined in an athymic rat model with a periodontal defect to see whether they could guide periodontal fiber orientation at the interface of root and ligament.<sup>[170]</sup> Cells transduced with AdBMP-7 were compared to nontransduced cells, and it was shown that the fiber-guiding structures successfully stimulated cell attachment and proliferation.<sup>[172]</sup> This methodology may be a starting point for the translational implementation of multiphased scaffold techniques in gingival tissue engineering.

The triphasic model was tested by Lee et al. using a conventional tissue engineering technique, including integrating scaffolds, bioactive compounds, and progenitor cells.<sup>[173]</sup> Porous patterns were altered to 3D print triphasic scaffolds of nanohydroxyapatite-PCL. Microchannels of 100, 300, and 600 µm were created to address the cementum/dentin contact, the alveolar bone, and the periodontal ligament, respectively.<sup>[173]</sup> Stem cells from tooth pulp were placed onto the scaffold and implanted subcutaneously into immunocompromised mice. Human amelogenin, bone morphogenetic protein-2, and connective tissue growth factor were used to modify the matrix layers for the cementum–dentin interaction, alveolar bone, and periodontal ligament, respectively.<sup>[173]</sup> Tissue formation was observed to be phase-specific, with the cementum/dentin phase displaying dense and polarized minerals, the periodontal ligament phase showing the formation of aligned fibrous matrix formation, and the bone phase revealing the generation of scattered minerals.<sup>[173]</sup> This evidence implies that multiphased and multilayered structures may efficiently guide tissue-specific formation through their optimized microstructure and spatiotemporal delivery of bioactive compounds.

One type of 3D printing is fused deposition modeling (FDM), whose application in engineering gingival soft tissues is yet to be reported. However, steps towards a more natural skin construct were achieved using FDM. This process involves melting a thermoplastic polymer and then depositing the molten polymer onto a surface or object using a heated extrusion nozzle. Benefits of this technology include high porosity without using hazardous solvents, excellent mechanical properties, and adaptability in operations and handling of materials.<sup>[174]</sup> Zein et al. showed that FDM could create scaffolds with tunable mechanical properties by controlling porosity and pore size. A bioresorbable poly (ε-caprolactone) (PCL) was used as a priming material to make a porous structure with interconnected honeycomb-like channels.<sup>[175]</sup> The primary constraint of FDM is its reliance on

premade filaments that must conform to the size and material specifications supplied to the nozzle. Further, FDM is limited to a select range of biodegradable polymers, such as PCL and polylactic acid (PLA).<sup>[176]</sup>

Chen et al. developed nanocomposite scaffolds using polyurethane (TPU)/polylactic acid (PLA)/graphene oxide (GO) as a result of the poor adhesion between layers in FDM; the printing orientation results in varied mechanical behavior. The 3D-printed scaffolds exhibit exceptional thermomechanical characteristics in addition to cell proliferation, allowing them to be widely employed in tissue engineering.<sup>[177]</sup> It is also shown that the porous PCL/HA scaffolds, in combination with 2 wt% carbon nanotubes (CNTs) developed by the FDM technique, have pore diameters between 450 and 750  $\mu\text{m}$ , increasing protein adsorption and cell adhesion.<sup>[178]</sup> Dong et al. developed a star-like PLA-heparin construct in another study. The construct's surface exhibited reduced platelet adhesion and protein adsorption while promoting increased fibroblast cell spreading compared to the construct without heparin. These observations highlight the potential of the scaffold for applications in tissue engineering of vascularized gingival constructs.<sup>[179]</sup>

Nonwoven membranes created by conventional electrospinning are formed of tightly packed nanofibers. This results in inappropriate cells spreading and growing into the core section of the scaffolds. Importantly, when it comes to artificial soft tissue like skin, conventional FDM can manufacture rigid materials. The high temperature of the FDM process also increases the risk of thermal degradation of materials. To address these limitations, combining electrospinning with FDM to create nano and microstructures was introduced in 2008, namely solvent exchange deposition modeling (SEDM).<sup>[180–181]</sup> Gao et al. used solvent exchange deposition modeling (SEDM) with electrospinning technology to develop a flexible bilayered nano-/microstructure to investigate its potential as a skin-like soft tissue replacement. The identical nozzle was utilized in both the SEDM and FDM processes; however, the shrinkage occurred during the FDM technique due to the immediate change from the melt to the solid phase.<sup>[182]</sup> Since the SEDM sample was tougher and had superior tensile strength than the fragile FDM sample, we may attribute these properties to the high temperature that may trigger the thermal breakdown of PLGA in the syringe. Cell proliferation and growth were also facilitated by the micro-sized pore between the strut fabricated by SEDM, indicating the scaffold potential for wound healing. Modifying the scaffolds with DOPA and EGF growth factors efficiently improved the healing procedure of full-thickness excisional skin wounds.<sup>[182]</sup>

### 4.3. 3D Bioprinting

Bioprinting is a promising field in tissue engineering that uses 3D printing technology to provide precise and controlled deposition of bioinks containing cells, growth factors, hormones, etc.<sup>[183–184]</sup> Bioprinting offers three main classes: extrusion-based bioprinting, laser-assisted bioprinting, and droplet-based bioprinting; in extrusion bioprinting, pressure is applied on a bioink to deposit filaments following a defined pattern.<sup>[185]</sup> Laser-assisted bioprinting (LAB) employs a laser as its energy source to precisely deposit biomaterials onto a substrate, and the droplet-

based method involves the deposition of bioink droplets through the printhead.<sup>[186]</sup>

Single-phasic scaffolds are simple and have applications, but they often fall short of replicating the complexity and functionality of native tissue. In contrast, biphasic or multiphasic scaffolds offer several advantages in mimicking native tissue and its structural characteristics. In tissue engineering, the terms “mono-phasic” and “bi/multiphasic” refer to the design and composition of engineered tissues or scaffolds. The engineered tissue or scaffold comprises a single homogeneous material or phase in a mono-phasic design. This means that the entire structure is composed of one type of material with uniform properties throughout. In contrast, a bi/multiphasic design incorporates two or more phases or materials within the tissue or scaffold structure. These layers can have varying properties, such as mechanical strength, porosity, or biochemical characteristics. Bi/multiphasic designs are often used to mimic the complexity of natural tissues, where different cell types or tissue components interact and contribute to overall function.

Extrusion-based bioprinting was used by Mangano et al. to create a mono-phasic scaffold consisting of HA,  $\beta$ -TCP, and  $\alpha$ -TCP.<sup>[187]</sup> Its distinguishing feature is a mesh-like structure, with an average of 300  $\mu\text{m}$  filament diameters and 60% microporosity with an average 370  $\mu\text{m}$  pore size. After 45 days of implantation in sheep sinus, the authors found that the immune system tolerated the scaffold, and full tissue integration and bone remodeling were achieved. A central area of highly vascularized fibrous tissue included fibroblasts and a well-organized system of capillaries and larger blood vessels. However, the scaffold biodegradation rate did not compromise new bone tissue formation since the scaffold slowly degraded after 90 days.<sup>[187]</sup> Kim et al. constructed a scaffold composed of PCL and HA with a combination of SDF1 (stromal cell-derived factor 1) and BMP-7.<sup>[188]</sup> The scaffold showed interconnected microchannels with 200  $\mu\text{m}$  diameter filled with SDF1, BMP7, and a collagen type 1 solution. After nine weeks, the results showed the regeneration of periodontal soft tissue and the formation of new bone at the interface. SDF1 and BMP7 are crucial in attracting endogenous cells, including mesenchymal stem cells and endothelial cells, promoting vascularization. BMP7 showed a significant role in the differentiation of osteoblasts and mineralization. This work underscores the vital role of cell recruitment and homing in achieving successful regeneration.<sup>[188]</sup>

The structural organization or cellular and biochemical composition of native tissue is often replicated, to some extent, in a multilayered scaffold, which can be defined by the variation within the design, including porosity, pore shape and size, and chemical/cellular composition.<sup>[189]</sup> Lee et al. conducted proof-of-concept research to demonstrate the feasibility of using extrusion-based bioprinting for soft (e.g., human skin) tissue applications. The dermis and epidermis of human skin vary in composition. This was mimicked in their work by depositing collagen, keratinocytes, and fibroblasts sequentially to develop a layer-by-layer scaffold.<sup>[190]</sup> In another study, Michael et al. developed full-thickness skin tissue by bioprinting fibroblasts in 20 layers, followed by keratinocytes in 20 layers onto a Matrigel platform. After 11 days of implantation in mice, full-thickness skin was formed that was firmly linked to the surrounding tissue.<sup>[191]</sup>



In addition to chemical and cellular composition variations, changing the physical and mechanical properties of the scaffold may provide a native tissue gradient structure. According to Ge and colleagues, the rate of fibroblast cell migration may be influenced by varying both the wavelength and amplitude of wavy patterns.<sup>[192]</sup> In contrast, Cheng et al. hypothesized that the sinusoidal wavy pattern slows endothelial cell migration rate. A square wave design provides the most significant cell migration speed, followed by a triangle wave structure. The migration rate for sinusoidal structures reduces even more when the wavelength increases.<sup>[193]</sup> Continuous gradient constructs are more effective than discrete multiphasic structures when regenerating soft to hard tissues.<sup>[194]</sup> A substance that has a stiffening gradient enables stress to be distributed at the interface and promotes cell migration.<sup>[195]</sup> Hu et al. observed that an increase in substrate stiffness led to a decrease in autophagy levels of vascular endothelial cells and a decrease in the expression of genes necessary for endothelial autophagy function. In another study, the autophagy levels of smooth muscle cells were found to increase under the influence of substrate stiffness.<sup>[196]</sup> Stiffness is a crucial factor in regulating cellular activities; however, the response to stiffness varies among cell types. MSCs are attracted to rigid surfaces. Fibroblasts and endothelial cells tend to migrate and proliferate in response to increased stiffness in their microenvironment. The ability of cells to undergo differentiation depends on their cell type and the stiffness of their environment. For instance, MSCs exhibit enhanced differentiation when exposed to rigid surfaces.<sup>[197]</sup> Research has demonstrated that a rigid scaffold promotes myogenic and osteogenic differentiation.<sup>[198]</sup>

## 5. Microfluidic Organ-on-Chip Systems

Alongside biofabrication methodologies, the advent of microfluidic organ-on-chip systems introduces enhanced conditions mimicking oral tissue, thereby offering advanced 3D models. These models facilitate a deeper comprehension of tissue functionality, drug responses, and pharmaceutical development. Fabricating gingival tissue constructs is a multistep process involving the 3D culture of keratinocytes and its culture at an air–liquid interface to promote epithelium stratification and differentiation.<sup>[87,95,199]</sup> Commercially available Transwell systems are conducive to performing cultures at the air–liquid interface and fabricating 3D organotypic gingival constructs under static culture conditions. Applying next-generation tools like microfluidic organ-on-a-chip systems provides unprecedented opportunities to emulate various microanatomical features of the gingiva and study the host-material and host-microbiome interactions under microphysiological flow conditions. These devices consist of microchannels or chambers that allow control of fluid flow, nutrient supply, and metabolic waste elimination, mimicking the role of vascular and interstitial tissue fluid flow in native tissues. The presence of media flow, environmental controls, integration of sensors, and downstream readout capabilities enables the emulation of the tissue-specific microenvironments. It allows cells to grow in a microarchitecture closely resembling *in vivo* conditions.<sup>[200]</sup>

The application of microfluidic technologies in emulating oral and dental barrier tissues is gaining significant traction.<sup>[17,201]</sup> The integration of organotypic cultures and fluid

dynamics using platforms such as perfusion bioreactors, oral mucosa-on-chip, gingival crevice-on-chip, gingiva-on-chip, gingival epithelial-capillary interface-on-chip, and tooth-on-chip has provided unprecedented opportunities to emulate microanatomical features of the gingiva, oral mucosa, and dental barrier tissues.<sup>[16,81,96,202–208]</sup> Design features of organ-on-a-chip systems play a pivotal role in shaping their capabilities, applications, and limitations. Customization of the design features facilitates the emulation of tissue microenvironments and their interface with internal and external factors. The microfluidic platforms for the biofabrication of oral mucosa and gingival barrier tissues typically have a configuration of a culture chamber sandwiched between two channels that are either horizontally or vertically stacked.<sup>[81,202,207–210]</sup>

Fluid flow has been shown to enhance the proliferation and metabolic activity of gingival fibroblasts and keratinocytes while also simulating the protective effects of gingival crevicular fluid flow and associated host innate immune responses.<sup>[81,211–212]</sup> The interstitial fluid within the gingival connective tissue contributes to the formation of gingival crevicular fluid (GCF), a protective factor against bacteria and by-products in the gingival crevice. To replicate this fluid flow, Makkar et al. developed a microfluidic device known as the gingival crevice-on-chip (**Figure 8A**).<sup>[81]</sup> This device features a microchamber flanked by tissue fluid (media) and crevicular (microbial) channels. Gingival connective tissue equivalents, composed of primary gingival fibroblasts in a 3D fibrin-based matrix, were cultured in the microchamber, and live oral bacteria were seeded into the crevicular (microbial) channel. The investigators simulated interstitial flow through the gingival connective tissue equivalents and GCF flow into the crevicular channel by establishing a hydrostatic pressure gradient between the channels. This design facilitated long-term host-microbe coexistence, microbial clearance emulation, and innate immune response modulation. Raub and colleagues employed a similar horizontally stacked three-channel design to culture oral mucosa constructs on-chip, shedding light on host-material and host-microbe interactions.<sup>[208,210]</sup> Though this design allowed real-time visualization of cells, collagen matrix contraction constrained prolonged culture and keratinocyte infiltration. Secondly, the lack of air–liquid interface culture limited the epithelial maturation, leading to an immature epithelial barrier.

Subsequent studies successfully mitigated collagen matrix contraction issues by optimizing fibroblast and collagen concentrations and ruthenium-catalyzed photocrosslinking to strengthen the collagen gel.<sup>[207,210]</sup> The optimized design was used to model the induction and recovery of chemotherapy and radiation-induced oral mucositis on-chip.<sup>[207]</sup> Similarly, the oral epithelial-capillary interface (**Figure 8B**) was recapitulated using a two-chambered PDMS microfluidic device.<sup>[202]</sup> Oral keratinocytes from explant cultures were cultured in monolayer in the top chamber and endothelial cells below. Inflammation was induced by exposure to LPS and TNF- $\alpha$ . Expression of cell adhesion molecules and beta-defensins were analyzed with and without the presence of NF-KB blocker, showcasing the use of a microfluidic model for testing anti-inflammatory therapeutics.

A nonleaky epithelial barrier is essential for the clinical translation of biofabricated gingival tissues, and the underlying extracellular matrix stiffness influences this property in the keratinocytes. Lee and colleagues utilized the organ-on-chip

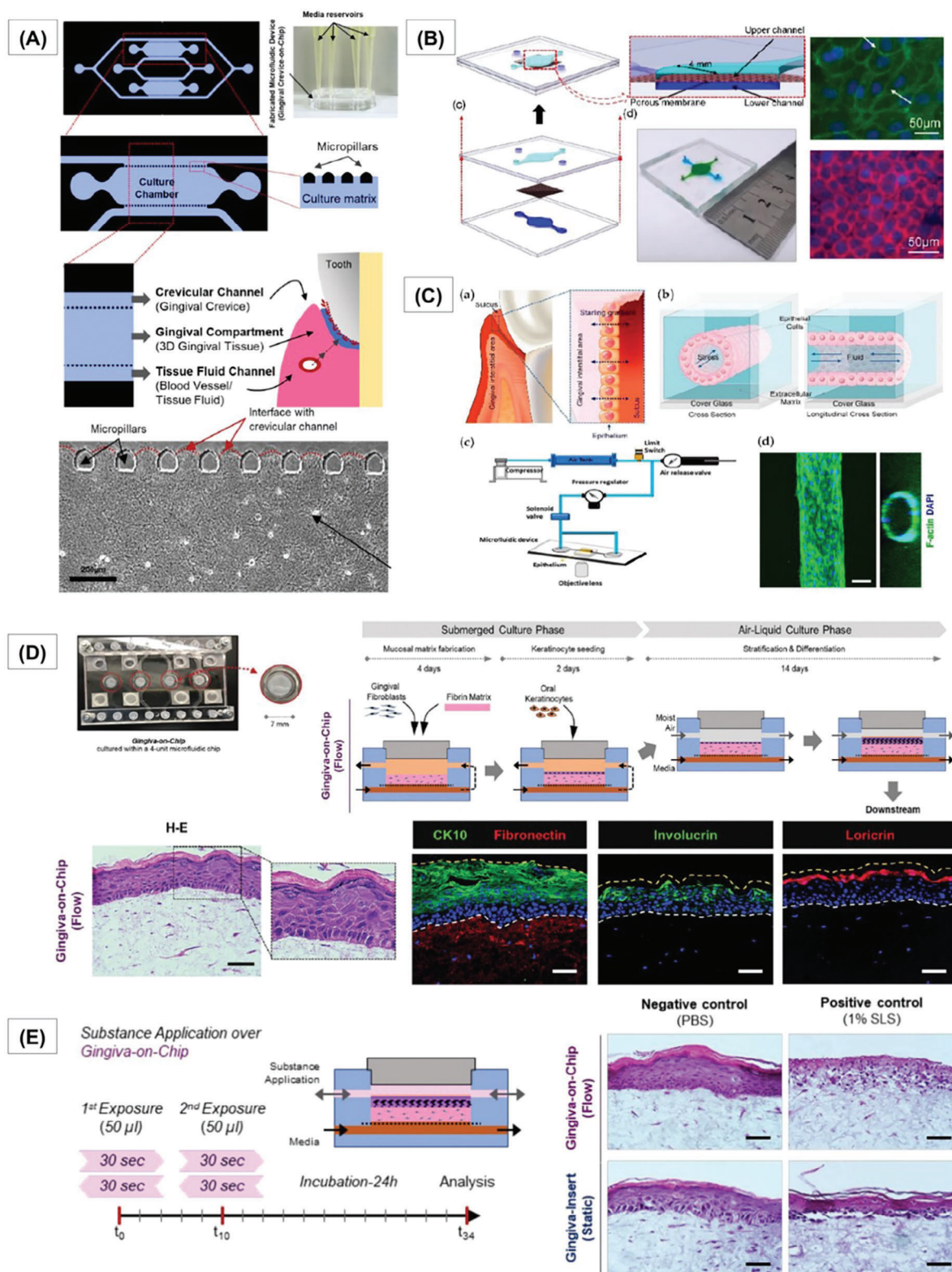


**Figure 8.** Emulating gingival tissues using microfluidic organ-on-chip systems. A) Design features of a gingival crevice-on-chip microfluidic device comprising a central culture chamber (gingival compartment) lined by microfluidic channels on either side representing the tissue fluid and crevicular channels. B) Design features of epithelium–capillary interface-on-a-chip comprising an upper (epithelial) and lower (endothelial) chamber separated by a porous membrane. C) Schematic depicting a cross-sectional area of the epi-mucosa-on-a-chip platform where oral keratinocytes are seeded in a 3D extracellular matrix within a microfabricated PDMS gasket and confocal immunofluorescence image capturing the formed epithelial cells stained for

technology to develop a model for studying the mechanical cues on the epithelial barrier properties (Figure 8C).<sup>[213]</sup> Using collagen as a representative ECM and modulation of its stiffness with the addition of fibronectin, they observed that intermediate matrix stiffness retained barrier properties. In contrast, soft and stiff matrices made the barrier leakier. Using a microfluidic organ chip platform, Muniraj et al. recently reported the biofabrication of full-thickness gingival equivalents under flow conditions. They integrated its downstream applications in toxicological and drug permeation studies (Figure 8D).<sup>[16]</sup> This microfluidic gingiva-on-chip platform was designed to emulate the intricate microenvironment of the gingiva and its application for the evaluation of host-material interactions and transmucosal permeation of oral-care products. Utilizing a vertically stacked microfluidic device that allows ALI culture, the gingiva-on-chip platform supports the biofabrication of full-thickness gingival equivalents with improved epithelial morphogenesis, maturation and barrier functionality under dynamic flow conditions compared to static cultures.

Interestingly, the microfluidic design and flow control features were used to replicate the mechanical action of mouth rinse. Despite the thicker and more mature epithelium in gingiva-on-chip cultures, the flow-induced exposure and mechanical rinsing of oral-care formulations lead to increased tissue disruption and cytotoxic effects compared to exposure under static conditions (Figure 8E). The results from these studies can influence the use of biomaterial and fabrication strategies for gingival tissue bioprinting, where incorporating these cues can affect the functionality of the epithelial barrier. Overall, the convergence of 3D biomaterial printing, bioprinting, and microfluidic technologies offers a promising avenue for precise control over the spatial and temporal arrangement of cells and extracellular matrix (ECM) components and the perfusion of larger tissue constructs. This can further pave the way towards designing and biofabrication of personalized gingival tissue constructs. Furthermore, incorporating larger bioprinted tissue constructs into perfusion-based bioreactors or microfluidic culture systems could address challenges related to tissue diffusion and enable long-term dynamic culture at the air-liquid interface, facilitating tissue maturation before their suitability for transplantation.<sup>[61,206,214–215]</sup>

## 6. Insights From Biofabrication of Skin Tissue Constructs

Skin is a complex and highly specialized multifaceted barrier tissue that protects against physical, chemical, and microbial agents, ensuring functions such as water retention, resistance to mechanical trauma, and protection against temperature, light, toxins, and microorganisms.<sup>[89,216]</sup> Beyond its protective role, the skin contributes to sensory perception, thermoregulation, excretion, absorption, pigmentation, and innate immunity.<sup>[216]</sup>

Barrier tissues at the interface with the external environment, skin, and gingiva share several similarities (Table 2). Briefly, the skin and gingiva are covered by keratinized stratified squamous epithelium termed epidermis and gingival epithelium. While the epidermis of the skin is supported by vascular dermal and hypodermal layers beneath, the gingival epithelium is supported by vascularized lamina propria.<sup>[89,220]</sup> A robust vasculature network in both tissues plays a crucial role in oxygen and nutrient supply, removal of metabolic wastes, immune response, and survival of the stratified squamous epithelial covering. In both tissues, the keratinized outer layer called stratum corneum forms a crucial barrier against physical, mechanical, chemical, and microbial agents.<sup>[216,220]</sup> In addition to its barrier role, the stratified epithelial and corneal layers form a semipermeable membrane that controls the permeability of water, electrolytes, and chemicals. The skin and gingival tissues are home to many commensal bacteria and encounter pathogenic bacteria. The barrier properties of the corneal layer, combined with the innate immune defense mechanisms of the skin and gingival tissues, form a barrier against the infiltration of commensal and pathogenic bacterial species.

Further, human skin produces antimicrobial peptides, such as cathelicidins and defensins, two prominent families of mammalian antimicrobial proteins.<sup>[221]</sup> These peptides play a vital role in the innate antimicrobial defense of the host by disrupting the integrity of bacterial cell membranes. Similarly, keratinized gingiva stabilizes the periodontium, shields the teeth and implants from external damage, and acts as a barrier against bacterial invasion. Despite these similarities, there are distinct differences between the two tissues, including microanatomical variations such as the presence of skin appendages like hair follicles, sweat glands, and sebaceous glands and distinct differences in wound healing responses. While wounds in the skin and oral mucosa (including gingiva) follow similar stages of healing, including hemostasis, inflammation, proliferation, and remodeling, oral mucosal injuries generally recover more quickly without a scar.<sup>[89]</sup> Despite oral and dermal fibroblast sub-populations being part of the broader adult fibroblast population, they exhibit marked phenotypic and functional variations that account for the distinct healing outcomes observed in these regions.<sup>[89,222–225]</sup>

The advances in tissue engineering and biofabrication techniques for skin tissues, encompassing the replication of multicellular architecture, vasculature, air-liquid interface culture, and crucial barrier features like keratinization and antibacterial properties, offer insights that can be leveraged for the biofabrication of gingival tissues. Ma et al. addressed the challenges of inadequate vascularization and poor angiogenesis in skin tissue engineering.<sup>[226]</sup> To do so, strontium silicate microstructures were incorporated into the bioink, promoting vascular network formation and angiogenesis in vitro and in vivo.<sup>[226]</sup> Similarly, 3D bioprinting through the incorporation of human dermal

F-actin. D) The image of the gingiva-on-chip microfluidic device and schematic show steps in the culture of full-thickness gingival equivalents under flow conditions. Brightfield and immunostained images of gingival equivalents show enhanced epithelial morphogenesis and expression of gingival maturation markers under flow conditions. E) Application of the gingiva-on-chip and fluidic control feature to emulate the rinsing effect of mouthwash and the potentially damaging impact of the mechanical action of mouthrinse on the gingival epithelium. (A), (B), (C), (D, E) Adapted from references,<sup>[81]</sup> Copyright 2022, John Wiley and Sons; open access article distributed under the terms and conditions of the Creative Commons Attribution (CC BY) license;<sup>[202]</sup> Copyright 2023, MDPI;<sup>[213]</sup> Copyright 2023, John Wiley and Sons, respectively.<sup>[16]</sup>

**Table 2.** Similarity of skin and gingival tissue.<sup>[217–219]</sup>

Features	Skin Tissue	Gingival Tissue
Histological Layers	Epidermis (keratinized stratified squamous epithelium), Dermis and Hypodermis	Epithelium (keratinized stratified squamous epithelium), Lamina propria covering the tooth surface/alveolar or palatal bone
Keratinization	Present in the outermost layer of epidermis (stratum corneum)	Present in the outermost layer of the epithelium (stratum corneum)
Epithelial Thickness	Varies in different body regions	Relatively thin ( $\approx 0.2$ – $0.4$ mm)
Pigmentation	Presence of melanocytes determines coloration	Pink or coral pink due to transparent epithelium transmitting the rich blood supply. Presence of melanocytes can alter the color.
Innervation	Richly innervated by sensory nerve fibers	Innervated by sensory nerve fibers
Vascularization	Highly vascularized with a dense capillary network	Rich blood supply through subepithelial plexus
Collagen Composition	Collagen types I and III predominate	Collagen types I and III predominate
Fibroblast Population	Abundant fibroblasts involved in ECM production, remodeling, and wound healing	Abundant fibroblasts involved in ECM production, remodeling and scarless wound healing
Immune Cells	Langerhans cells, neutrophils, lymphocytes	Langerhans cells, neutrophils, lymphocytes
Attachment	Epidermis is firmly anchored to underlying dermis through basement membrane	Epithelium is firmly anchored to underlying lamina propria through basement membrane
Regenerative Capacity	Moderate regenerative capacity	Excellent regenerative capacity
Healing Response	Scar formation upon injury or surgery	Scarless healing. However, the interface with the tooth can heal with the formation of long junctional epithelium.
Function	Protection, temperature regulation, sensation	Protection, masticatory support, sensation

fibroblast cells, pericytes, and endothelial cells encapsulated in collagen type I bioink for dermis and human keratinocytes encapsulated in collagen type I bioink for epidermis demonstrated remarkable *in vitro* microvessel formation in the dermis and enhanced epidermal development (Figure 9A).<sup>[227]</sup> In addition, an *in vivo* study using mouse skin wounds showed early graft integration and perfusion due to anastomosis with the mouse vasculature (Figure 9B).<sup>[227]</sup> Another study utilized extrusion-based and inkjet bioprinting methods to fabricate a prevascularized skin construct, in which decellularized porcine skin-based bioink was incorporated with human epidermal keratinocytes, dermal fibroblasts, endothelial progenitor cells, and human adipose tissue-derived mesenchymal stem cells (Figure 9C).<sup>[228]</sup> The decellularized skin-based bioink accelerated and improved upon vascularization compared to the collagen-based bioink. The resulting skin construct is effectively re-epithelialized, vascularized, and anastomosed with the host vascular network, resulting in wound closure, proving the critical role of bioink and encapsulated cells in vascular tissue bioprinting.<sup>[229]</sup>

The effectiveness of biomaterials and scaffolds for skin tissue engineering in preventing the growth and dissemination of pathogens is critical for averting infections and related diseases. This feature is equally important from the perspective of gingival tissue regeneration owing to the constant influx of bacterial load. Afghah et al. developed biocompatible and biodegradable polycaprolactone and propylene succinate-based scaffolds incorporating silver particles, providing antibacterial properties.<sup>[231]</sup> The scaffolds' potential for hydrolysis and enzymatic degradation was improved. Silver particles inhibited the spread of bacteria infecting the scaffold. Authors noted that using 3D bioprinting provided the feasibility of controlling degradation be-

havior and antibacterial activity, paving the way for tissue engineering and wound healing.<sup>[231]</sup> In addition to its notable antibacterial attributes, the skin's intrinsic permeability and barrier characteristics are crucial elements in its multifaceted role as a protective interface between the body and the external environment. While the skin's antimicrobial defenses are instrumental in averting pathogenic threats, the stratum corneum plays a pivotal role as the primary barrier against microbes and functions as a semipermeable barrier membrane for the penetration, absorption, and transport of chemical substances. The stratum corneum, comprising densely packed corneocytes embedded within a lipid matrix, creates a formidable barrier against the ingress of exogenous agents, mitigating trans-epidermal water loss, safeguarding against external stressors, and preserving physiological homeostasis.<sup>[232–234]</sup> Innovative approaches using microfluidic organ-on-chip systems and 3D bioprinting have revolutionized the biofabrication of skin constructs, focusing on enhancing the vital role of the stratum corneum and barrier function. Utilizing microfluidic skin-on-chip with controlled media and air flow-induced mechanotransduction signals, Sriram et al. demonstrated the fabrication of skin constructs with improved epidermal morphogenesis, enhanced differentiation, and superior barrier function compared to conventional static cultures.<sup>[232]</sup> The stratum corneum's enhanced epidermal differentiation and maturation were evidenced by the lower water content and higher keratin content in the stratum corneum, which translated to enhanced transepidermal electrical resistance and lower permeation of compounds.

Further, differences in air-lift phase duration and culture medium supplementation significantly impact stratum corneum thickness and composition.<sup>[233]</sup> In gingival tissues, the stratum

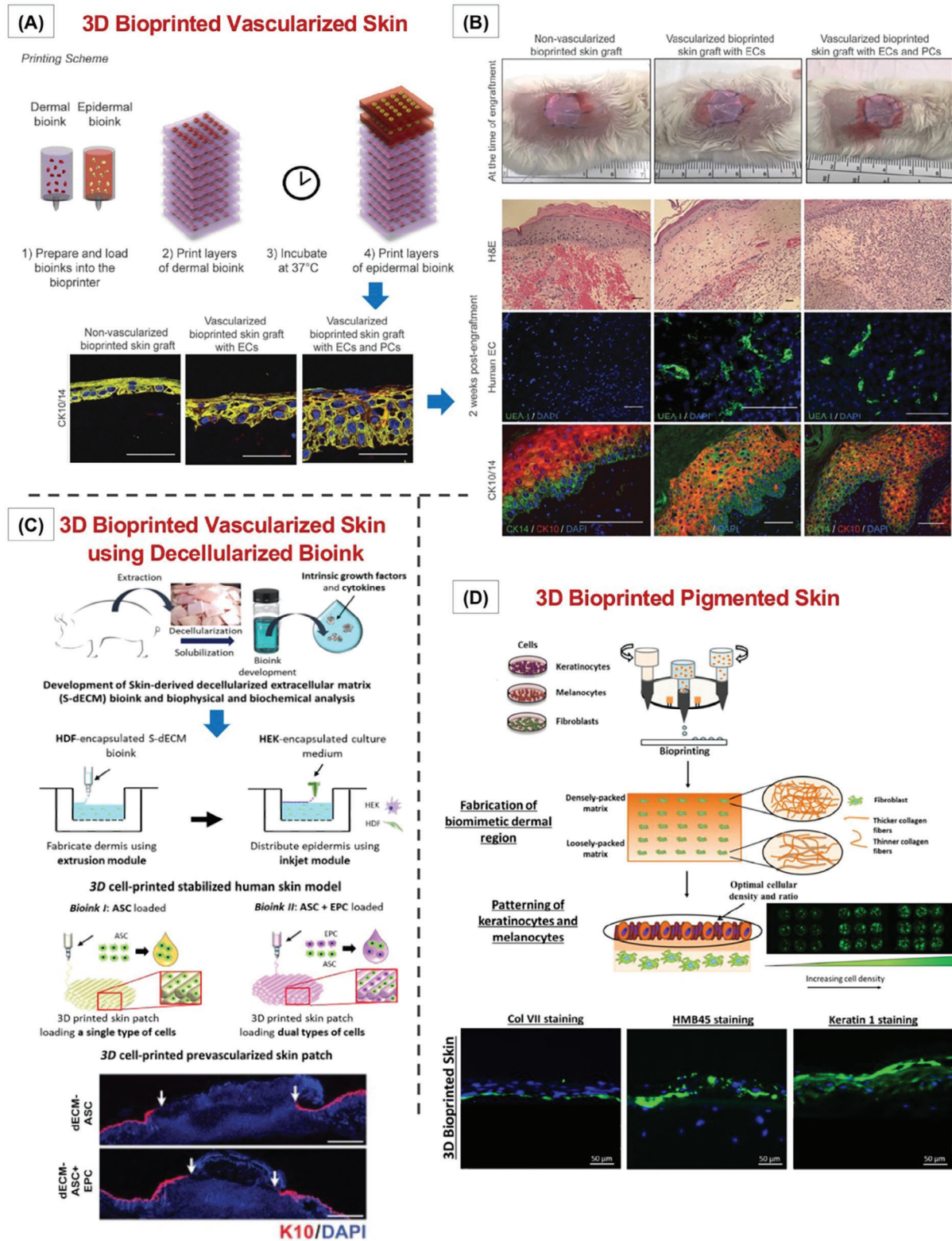


**Figure 9.** 3D bioprinting-based biofabrication of multicellular vascularized and pigmented skin constructs. A, B) 3D bioprinting of full-thickness vascularized skin equivalent and its engraftment onto immunodeficient mice. C) Biofabrication of vascularized skin equivalents using a porcine skin-derived decellularized extracellular matrix bioink and its impact on enhanced wound healing. D) Proof of concept 3D bioprinting of pigmented human skin equivalents using keratinocytes, melanocytes, and fibroblasts, and immunofluorescence images showing the expression of basement membrane (Col VIII), melanocyte (HMB45) and epithelial (keratin 1) markers. (A, B), (C), (D) Adapted from references, Copyright 2020, Mary Ann Liebert, Inc.;<sup>[227]</sup> Copyright 2018, Elsevier;<sup>[228]</sup> Copyright 2018, IOP Publishing, respectively.<sup>[230]</sup>

corneum plays a significant role as a primary barrier against microbes and chemical substances, and insights from in vitro skin platforms have been recently cross-applied. Similar to the findings on microfluidic skin-on-chip, reconstruction of gingival equivalents under flow conditions (gingiva-on-chip) showed a flow-induced enhancement in the morphogenesis, maturation, and barrier properties of the gingival epithelium.<sup>[16]</sup> In addition, the transepithelial transport of tissue fluid (gingival crevicular fluid) from the gingival connective tissue into the gingival sulcus further contributes to microbial defense.<sup>[81,235]</sup> These protective effects of the gingival tissue against the oral microbiome were recently demonstrated using a microfluidic gingival crevice-on-chip, wherein the mechanical flushing action of gingival crevicular fluid flow and its modulation of the innate immune response against periodontopathogens was shown.<sup>[81]</sup>

Derr et al. bioprinted a skin tissue that mimics the shape and barrier function. Neonatal human dermal fibroblasts were encapsulated in gelatin-fibrinogen-collagen type I-elastin bioink to engineer the dermis. A thin layer of entactin and laminin was bioprinted for the basal membrane, and human keratinocytes were bioprinted as a cellular coating on top. The barrier function was demonstrated by electrical impedance and permeability testing.<sup>[236]</sup> Ilhan and her colleagues studied permeable porous wound dressing using 3D bioprinting to address challenges related to acute wounds.<sup>[237]</sup> In this research, diabetic foot ulcers were successfully treated using a plant extract from the *Satureja cuneifolia* plant. The extract was combined with sodium alginate and polyethylene glycol bioinks. The adequate extract permeation resulted in an antimicrobial effect when scaffolds were tested with some topical bacteria strains. The findings were identical to those of the ampicillin antibiotic administered as a control in the wound healing procedure. This indicated the potential of the design for soft tissue engineering, such as gingiva.<sup>[237]</sup>

It is demonstrated that 3D bioprinting makes creating dermis and epidermis structures with a cellular architecture feasible. Pourchet et al. studied a gelatin-alginate-fibrinogen bioink.<sup>[238]</sup> The skin tissue with 5mm thickness was bioprinted. Keratinocytes were added using desmosomes that contain intracellular keratin filaments and compartments. Desmosomes-connected keratinocytes are essential for epidermal regeneration. These hemidesmosomes were associated with the keratin filaments laden in basal keratinocytes. It should be noted that the only known method capable of producing a 5 mm thick dermis is seeding cells onto a collagen-based sponge. Using bioprinting allows the fabrication of complicated structures, which can be translated into gingival tissue biofabrication.<sup>[238]</sup>

A two-step droplet-based bioprinting method developed hierarchical porous skin scaffolds containing melanocytes and keratinocytes (Figure 9D). The cells were placed in designated positions, mimicking the native human pigmentation.<sup>[230]</sup> A heterogeneous epidermal model may be created using a patterned bioprinting technique. Thanks to a semicircle architecture, two distinct keratinocyte populations can be found in a single insertion.<sup>[239]</sup> In one study, cross-linkable collagen bioink was initially used to inkjet bioprint human dermal fibroblasts, then bioprint human melanocytes and keratinocytes. Air-liquid exposure induced stratification of keratinocytes, generating freckle-shaped pigmented structures.<sup>[240]</sup> In a similar strategy, the 3D bioprinted skin structure exhibited a more developed stratifi-

cation of epidermal and a continuous basement membrane layer than the conventionally molded skin structure.<sup>[230]</sup> The fibrinogen-collagen bioink containing human fibroblasts inkjet bioprinted dermis-like structure that was promptly crosslinked with subsequent thrombin deposition. Keratinocytes were then bioprinted on top of the scaffold. In vivo results showed a full-thickness wound repair.<sup>[241]</sup>

Lastly, it is imperative to consider the modalities to visualize the cellular and extracellular components of the biofabricated gingival constructs during the culture and maturation phase to monitor the cellular viability, proliferation, maturation, and functionalities. While conventional histological methods are the gold standard for visualizing and analyzing cellular and matrix organization, they are time-consuming, resource-intensive, and provide only cross-sectional information in time and spatial architecture. To that end, various 3D imaging and noninvasive modalities like confocal laser scanning, confocal reflectance, two/multiphoton and second harmonic generation, confocal Raman spectroscopy, and light sheet microscopy have been utilized in clinical and experimental dermatology (Figure 10A–E).<sup>[88,232–233,242–249]</sup> These imaging tools have provided an opportunity for label-free and noninvasive imaging of cellular and matrix components in 3D space that could be referred to as optical biopsy, in contrast to 2D histological images. These imaging technologies have been applied in oral mucosal biology, such as the use of two/multiphoton microscopy to visualize the keratinocytes, fibroblasts and collagen fibers (Figure 10A,B);<sup>[88,124,250]</sup> confocal reflectance microscopy to visualize fibroblasts, vasculature and extracellular matrix components within the gingival connective tissue equivalents (Figure 10C);<sup>[92,123]</sup> and light sheet microscopy to visualize vascular networks within the human gingiva (Figure 10E).<sup>[251]</sup>

## 7. Future Directions and Conclusions

The present review explores the challenges surrounding gingival recession, a prevalent oral health concern. We initiate by describing the limitations of prevalent surgical approaches, emphasizing the pressing need for alternative biofabrication strategies to advance traditional treatments and push the field of gingival tissue engineering forward. Despite its vast promise, tissue engineering in periodontal regenerative therapies is in its early stages. Researchers and clinicians focus on achieving optimal structural materials, mimicking intricate microenvironments, and ensuring vascularization and integration to unlock their full potential. In the subsequent section of the review, we explored some of the critical biomaterial, cellular, and biological factors to be considered, such as porosity, mechanical properties, permeability, biodegradability, different cell lines employed, and biomimetic extracellular matrix components—all integral for achieving optimal tissue integration and facilitating effective regeneration. In the third part of the review, we thoroughly detail electrospinning, 3D biomaterial printing, and 3D bioprinting—biofabrication technologies that have shown remarkable potential in promoting vasculature development and tissue regeneration in preclinical models. The combination of models aligned with advancements in precision, material science, and the integration of biological cues can revolutionize periodontal regenerative therapies by providing personalized, structurally accurate

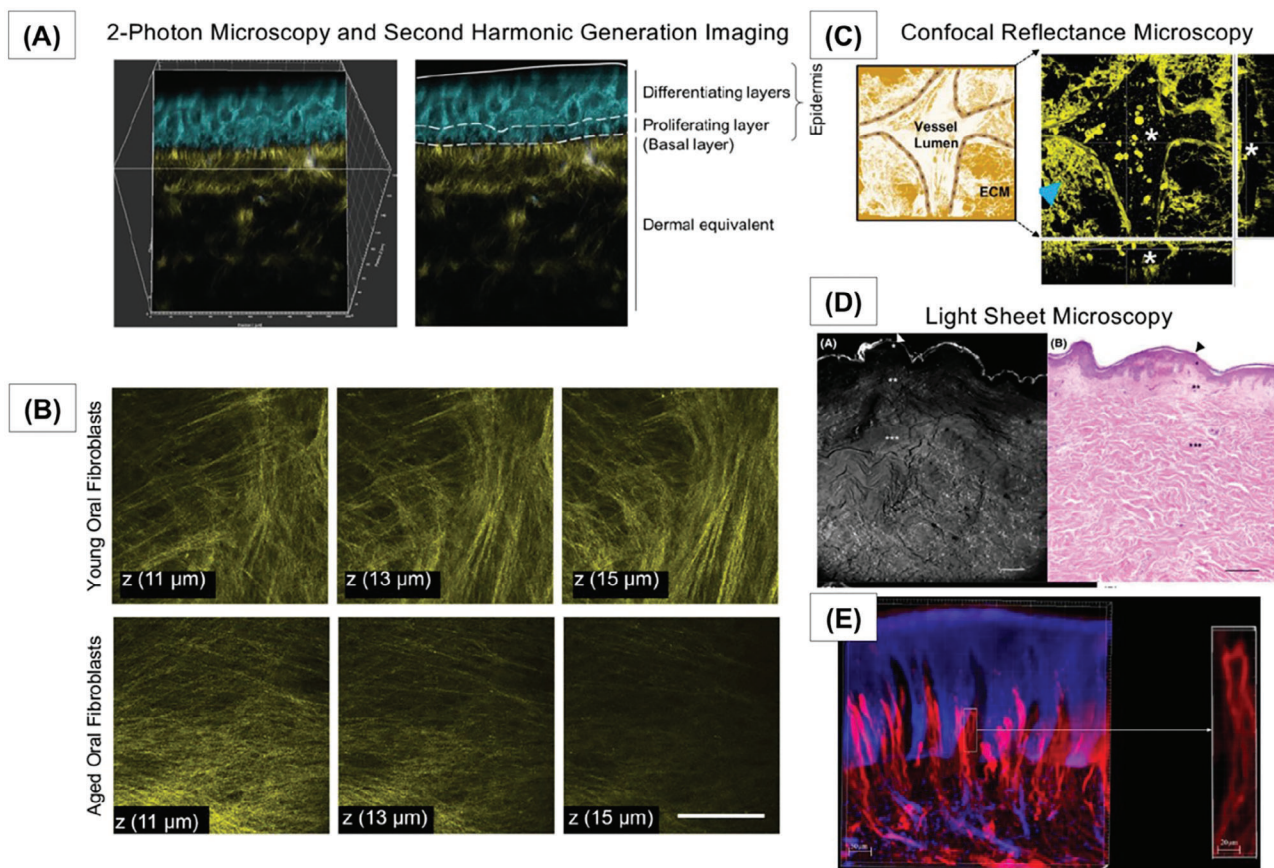


**Figure 10.** Noninvasive imaging tools to visualize the cellular and extracellular components. A) Label-free multiphoton microscopy of biofabricated full-thickness skin equivalents reveals the proliferating and differentiated layers of the epidermis represented by 2-photon excited fluorescence (2PEF) from nicotinamide adenine dinucleotides (NADH) within keratinocytes (*cyan*) and second harmonic generation (SHG) imaging of collagen fibers (*yellow*) within the dermal layer. B) Label-free SHG imaging demonstrates the differences in the organization of collagen secreted by young and aged oral mucosal fibroblasts. C) Label-free confocal reflectance microscopy of biofabricated vascularized gingival connective tissue equivalent showing a trifurcated vessel with lumen. D) Light-sheet microscopic Imaging of human skin following optical clearing compared to H&E image. E) Light-sheet microscopy of human gingiva embedded in agarose with CD31-positive blood vessels (*red*). (A), (B), (C), (D), (E) Adapted from references Copyright 2019, Springer;<sup>[88]</sup> Copyright 2020, John Wiley and Sons;<sup>[124]</sup> Copyright 2023, IOP Publishing;<sup>[123]</sup> Copyright 2018, John Wiley and Sons;<sup>[248]</sup> Copyright 2018, Springer Nature, respectively.<sup>[251]</sup>

constructs that could substantially reduce recovery periods and surgical interventions.

To conclude, we establish parallels between skin and gingiva, highlighting their shared characteristics as barrier tissues with similar cellular structures. Thus, learning from the advancements in skin tissue engineering can significantly influence the biofabrication of gingival tissues, specifically by replicating skin's antimicrobial defenses, stratum corneum properties, and barrier function through bioprinting and microfluidic platforms, offering an outline for enhancing the functionality of biofabricated gingival tissues.<sup>[252–257]</sup> The advancements covered herein pave the way for better tissue regeneration and hold tremendous potential for personalized medicine and disease modeling in regenerative dentistry.

## Acknowledgements

This project was supported by funding from the National Institutes of Health (NIH, National Institute of Dental and Craniofacial Re-

search [R01DE031476 to MCB] and National Institute of General Medical Sciences [R01GM143938 to MCB]). This work was partially supported by grants to GS from National University Healthcare System and Singapore Ministry of Education through NUHS Internal Grant Funding under its funding scheme (NUHS RO Project No. NUHSRO/2021/107/RO5+6/Seed-Sep/10; A-8000164-00-00. The authors apologize to those authors whose work may have been relevant to this review but was not cited due to a perceived lack of fit or due to space limitations. The content is solely the responsibility of the authors and does not necessarily represent the official views of the National Institutes of Health.

## Conflict of Interest

The authors declare no conflict of interest.

## Keywords

biofabrication, bioprinting, gingival recession, regeneration, skin, tissue engineering

Received: December 19, 2023  
Revised: March 1, 2024  
Published online: April 11, 2024

- [1] M. Nazir, A. Al-Ansari, K. Al-Khalifa, M. Alhareky, B. Gaffar, K. Almas, *Sci. World J.* **2020**, 2020, 2146160.
- [2] V. S. Yadav, B. Gumber, K. Makker, V. Gupta, N. Tewari, P. Khanduja, R. Yadav, *Oral Dis.* **2023**, 29, 2993.
- [3] M. M. Kassab, R. E. Cohen, *J. Am. Dent. Assoc.* **2003**, 134, 220.
- [4] J.-C. Imber, A. Kasaj, *Int. Dent. J.* **2021**, 71, 178.
- [5] L. Tavelli, S. Barootchi, M. Stefanini, G. Zucchelli, W. V. Giannobile, H. L. Wang, *Periodontol. 2000* **2023**, 92, 90.
- [6] G. Zucchelli, L. Tavelli, M. K. McGuire, G. Rasperini, S. E. Feinberg, H. L. Wang, W. V. Giannobile, *J. Periodontol.* **2020**, 91, 9.
- [7] S. Romeed, *Dent. Update* **2022**, 49, 584.
- [8] K. Izumi, H. Kato, S. E. Feinberg, in *Stem Cell Biology and Tissue Engineering in Dental Sciences*, Elsevier, Amsterdam **2015**.
- [9] O. Zühr, D. Baumer, M. Hürzeler, *J. Clin. Periodontol.* **2014**, 41, S123.
- [10] C. Lahham, M. A. Ta'a, *Heliyon* **2022**, e10132.
- [11] B. T. Yilmaz, E. Comerdiv, C. Kutuk, J. Nart, H. G. Keceli, *Clin. Oral Investig.* **2022**, 26, 6283.
- [12] G. Lauer, *J. Craniomaxillofac. Surg.* **1994**, 22, 18.
- [13] M. Klausner, Y. Handa, S. Aizawa, *In Vitro Cell Dev. Biol. Anim.* **2021**, 57, 148.
- [14] K. Moharamzadeh, H. Colley, C. Murdoch, V. Hearnden, W. L. Chai, I. M. Brook, M. H. Thornhill, S. Macneil, *J. Dent. Res.* **2012**, 91, 642.
- [15] K. Moharamzadeh, I. M. Brook, R. Van Noort, A. M. Scutt, M. H. Thornhill, *J. Dent. Res.* **2007**, 86, 115.
- [16] G. Muniraj, R. H. S. Tan, Y. Dai, R. Wu, M. Alberti, G. Sriram, *Adv. Healthcare Mater.* **2023**, 12, e2301472.
- [17] C. Huang, F. Sanaei, W. P. R. Verdurmen, F. Yang, W. Ji, X. F. Walboomers, *J. Dent. Res.* **2023**, 102, 364.
- [18] S. Bhargava, J. M. Patterson, R. D. Inman, S. MacNeil, C. R. Chapple, *Eur. Urol.* **2008**, 53, 1263.
- [19] M. Mohammadi, R. Mofid, M. A. Shokrgozar, *Acta Med. Iran* **2011**, 49, 319.
- [20] A. R. Stone, *Eur. Urol.* **2008**, 53, 1270.
- [21] S. Gupta, P. Pratibha, R. Gupta, *Dentistry* **2015**, 5, 2161.
- [22] Y. Ma, L. Xie, B. Yang, W. Tian, *Biotechnol. Bioeng.* **2019**, 116, 452.
- [23] M. Rahimnejad, F. Rasouli, S. Jahangiri, S. Ahmadi, N. Rabiee, M. Ramezani Farani, O. Akhavan, M. Asadnia, Y. Fatahi, S. Hong, J. Lee, J. Lee, S. K. Hahn, *ACS Biomater. Sci. Eng.* **2022**, 8, 5038.
- [24] S. V. Murphy, A. Atala, *Nat. Biotechnol.* **2014**, 32, 773.
- [25] H. E. Schroeder, M. A. Listgarten, *Periodontol. 2000* **1997**, 13, 91.
- [26] M. To, Y. Kamata, J. Saruta, T. Shimizu, T. Sato, Y. Kondo, T. Hayashi, N. Hamada, K. Tsukinoki, *Acta Histochem. Cytochem.* **2013**, 46, 25.
- [27] O. Karatas, H. Balci Yuçe, M. M. Taskan, F. Gevrek, E. Lafci, H. Kasap, *Acta Odontol. Scand.* **2020**, 78, 241.
- [28] S. Torabi, A. Soni, **2021**.
- [29] I. Farooq, S. Ali, P. Anderson, *An Illustrated Guide to Oral Histology*, Wiley, Hoboken, NJ **2021**.
- [30] A. R. Hand, M. E. Frank, *Fundamentals of Oral Histology and Physiology*, Wiley Blackwell, Ames, Iowa **2014**.
- [31] M. Bath-Balogh, M. J. Fehrenbach, P. Thomas, *Illustrated Dental Embryology, Histology, and Anatomy*, Elsevier Saunders, St. Louis, Mo **2006**.
- [32] S. Gibbs, S. Roffel, M. Meyer, A. Gasser, *Eur. Cell Mater.* **2019**, 38, 63.
- [33] Q. Jiang, Y. Yu, H. Ruan, Y. Luo, X. Guo, *BMC Oral Health* **2014**, 14, 30.
- [34] S. Hatakeyama, T. Yaegashi, Y. Oikawa, H. Fujiwara, T. Mikami, Y. Takeda, M. Satoh, *J. Periodontal Res.* **2006**, 41, 322.
- [35] S. Groeger, J. Meyle, *Front. Immunol.* **2019**, 10, 208.
- [36] I. C. Mackenzie, G. Rittman, Z. Gao, I. Leigh, E. B. Lane, *J. Periodontal Res.* **1991**, 26, 468.
- [37] T. Fatima, Z. Khurshid, A. Rehman, E. Imran, K. C. Srivastava, D. Shrivastava, *Molecules* **2021**, 26.
- [38] Y. Abiko, M. Saitoh, M. Nishimura, M. Yamazaki, D. Sawamura, T. Kaku, *Med. Mol. Morphol.* **2007**, 40, 179.
- [39] X. Li, D. Duan, J. Yang, P. Wang, B. Han, L. Zhao, S. Jepsen, H. Dommisch, J. Winter, Y. Xu, *Arch. Oral Biol.* **2016**, 66, 15.
- [40] Z. Abpeikar, A. A. Alizadeh, Y. Ahmadyousefi, A. A. Najafi, M. Safaei, *Regen. Med.* **2022**, 17, 855.
- [41] Q. L. Loh, C. Choong, *Tissue Eng., Part B: Rev.* **2013**, 19, 485.
- [42] H. Y. Jin, Y. Zhuo, Y. Sun, H. Y. Fu, Z. Y. Han, *Adv. Mech. Eng.* **2019**, 11, 1687814019883784.
- [43] V. Mastrullo, W. Cathery, E. Velliou, P. Madeddu, P. Campagnolo, *Front. Bioeng. Biotechnol.* **2020**, 8, 188.
- [44] A. A. Ayoub, A. H. Mahmoud, J. S. Ribeiro, A. Daghreery, J. Xu, J. C. Fenno, A. Schwendeman, H. Sasaki, R. Dal-Fabbro, M. C. Bottino, *Int. J. Mol. Sci.* **2022**, 23, 13761.
- [45] S. Goktas, J. J. Dmytryk, P. S. McFetridge, *J. Periodontol.* **2011**, 82, 1178.
- [46] P. A. Tran, *Mater. Lett.* **2021**, 285, 129184.
- [47] M. Rahimnejad, N. Nasrollahi Boroujeni, S. Jahangiri, N. Rabiee, M. Rabiee, P. Makvandi, O. Akhavan, R. S. Varma, *Nanomicro. Lett.* **2021**, 13, 182.
- [48] H. Tabesh, Z. Elahi, Z. Amoabediny, F. Rafiei, *Biomed. Res. Int.* **2022**, 2022, 1.
- [49] J. E. Jeon, C. Vaquette, T. J. Klein, D. W. Hutmacher, *Anat. Rec.* **2014**, 297, 26.
- [50] B. R. Freedman, D. J. Mooney, *Adv. Mater.* **2019**, 31, 1806695.
- [51] J. Chen, R. Ahmad, W. Li, M. Swain, Q. Li, *J. R. Soc., Interface* **2015**, 12, 20150325.
- [52] S. Ghanaati, M. Schlee, M. J. Webber, I. Willershausen, M. Barbeck, E. Balic, C. Gorch, S. I. Stupp, R. A. Sader, C. J. Kirkpatrick, *Biomed. Mater.* **2011**, 6, 015010.
- [53] D. Nestic, S. Durual, L. Marger, M. Mekki, I. Sailer, S. S. Scherrer, *Int. J. Bioprint.* **2020**, 20, e00100.
- [54] C. Vallecillo, M. Toledano-Osorio, M. Vallecillo-Rivas, M. Toledano, R. Osorio, *Polymers* **2021**, 13, 2633.
- [55] A. Paradowska-Stolarz, M. Wieckiewicz, A. Owczarek, J. Wegzowiec, *Int. J. Mol. Sci.* **2021**, 22, 10337.
- [56] C. W. Cheah, N. M. Al-Namnam, M. N. Lau, G. S. Lim, R. Raman, P. Fairbairn, W. C. Ngeow, *Materials* **2021**, 14, 6123.
- [57] J. J. E. Choi, J. Zwirner, R. S. Ramani, S. Ma, H. M. Hussaini, J. N. Waddell, N. Hammer, *Clin. Exp. Dent. Res.* **2020**, 6, 602.
- [58] M. H. Lacoste-Ferre, P. Demont, J. Dandurand, E. Dantras, D. Duran, C. Lacabanne, *J. Mech. Behav. Biomed. Mater.* **2011**, 4, 269.
- [59] H. Alghamdi, N. Babay, A. Sukumaran, *Saudi Dent. J.* **2009**, 21, 83.
- [60] J. C. Imber, A. Kasaj, *Int. Dent. J.* **2021**, 71, 178.
- [61] S. H. Mathes, L. Wohlwend, L. Uebersax, R. von Mentlen, D. S. Thoma, R. E. Jung, C. Gorch, U. Graf-Hausner, *Biotechnol. Bioeng.* **2010**, 107, 1029.
- [62] F. Berton, D. Porrelli, R. Di Lenarda, G. Turco, *Nanomaterials* **2019**, 10, 16.
- [63] R. Ophof, J. C. Maltha, A. M. Kuijpers-Jagtman, J. W. Von den Hoff, *Eur. J. Orthod.* **2007**, 30, 1.
- [64] M. Yoshizawa, T. Koyama, T. Kojima, H. Kato, Y. Ono, C. Saito, *J. Oral Maxillofac. Surg.* **2012**, 70, 1199.
- [65] R. Fernández-Valadés-Gómez, I. Garzón, E. Liceras-Liceras, A. España-López, V. Carriel, M. Martin-Piedra, M. Muñoz-Miguelsanz, M. C. Sánchez-Quevedo, M. Alaminos, R. Fernández-Valadés, *Biomed. Mater.* **2016**, 11, 015015.
- [66] J.-L. Roh, H. Jang, J. Lee, E. H. Kim, D. Shin, *Oral Oncol.* **2017**, 69, 84.



- [67] S. M. Lien, L. Y. Ko, T. J. Huang, *Acta Biomater.* **2009**, *5*, 670.
- [68] J. Rnjak-Kovacina, S. G. Wise, Z. Li, P. K. Maitz, C. J. Young, Y. Wang, A. S. Weiss, *Biomaterials* **2011**, *32*, 6729.
- [69] C. M. Murphy, M. G. Haugh, F. J. O'Brien, *Biomaterials* **2010**, *31*, 461.
- [70] S. Nehrer, H. A. Breinan, A. Ramappa, G. Young, S. Shortkroff, L. K. Louie, C. B. Sledge, I. V. Yannas, M. Spector, *Biomaterials* **1997**, *18*, 769.
- [71] S. J. Lee, I. W. Lee, Y. M. Lee, H. B. Lee, G. Khang, *J. Biomater. Sci. Polym. Ed.* **2004**, *15*, 1003.
- [72] D. Baksh, J. E. Davies, S. Kim, *J. Mater. Sci. Mater. Med.* **1998**, *9*, 743.
- [73] G. Akay, M. A. Birch, M. A. Bokhari, *Biomaterials* **2004**, *25*, 3991.
- [74] Y. Kuboki, Q. Jin, H. Takita, *J. Bone Joint Surg. Am.* **2001**, *83-A*, S105.
- [75] O. Oliviero, M. Ventre, P. A. Netti, *Acta Biomater.* **2012**, *8*, 3294.
- [76] L. R. Madden, D. J. Mortisen, E. M. Sussman, S. K. Dupras, J. A. Fugate, J. L. Cuy, K. D. Hauch, M. A. Laflamme, C. E. Murry, B. D. Ratner, *Proc. Natl. Acad. Sci. USA* **2010**, *107*, 15211.
- [77] G. S. Offeddu, L. Mohee, R. E. Cameron, *J. Mater. Sci.: Mater. Med.* **2020**, *31*, 46.
- [78] O. Moreno-Arotzena, J. G. Meier, C. Del Amo, J. M. Garcia-Aznar, *Materials* **2015**, *8*, 1636.
- [79] C. L. Chiu, V. Hecht, H. Duong, B. Wu, B. Tawil, *BioRes. Open Access* **2012**, *1*, 34.
- [80] S. P. Barros, R. Williams, S. Offenbacher, T. Morelli, *Periodontol. 2000* **2016**, *70*, 53.
- [81] H. Makkar, Y. Zhou, K. S. Tan, C. T. Lim, G. Sriram, *Adv. Healthcare Mater.* **2023**, *12*, e2202376.
- [82] B. C. W. Webb, M. Glogauer, J. P. Santerre, *Int. J. Mol. Sci.* **2022**, *23*, 5256.
- [83] K. Kobayashi, T. Suzuki, Y. Nomoto, Y. Tada, M. Miyake, A. Hazama, I. Wada, T. Nakamura, K. Omori, *Biomaterials* **2010**, *31*, 4855.
- [84] R. Leszczynski, E. Stodolak, J. Wiecek, J. Orłowska-Heitzman, T. Gumula, S. Blazewicz, *J. Mater. Sci. Mater. Med.* **2010**, *21*, 2843.
- [85] A. P. Strange, UCL University College London, **2019**.
- [86] J. Caballe-Serrano, S. Zhang, A. Sculean, A. Staehli, D. D. Bosshardt, *Materials* **2020**, *13*, 2420.
- [87] A. Dongari-Bagtzoglou, H. Kashleva, *Nat. Protoc.* **2006**, *1*, 2012.
- [88] G. Sriram, T. Sudhaharan, G. D. Wright, *Methods Mol. Biol.* **2020**, *2150*, 195.
- [89] G. Sriram, P. L. Bigliardi, M. Bigliardi-Qi, *Eur. J. Cell Biol.* **2015**, *94*, 483.
- [90] E. M. Lu, C. Hobbs, M. Ghuman, F. J. Hughes, *J. Periodontal Res.* **2021**, *56*, 147.
- [91] E. M. Lu, C. Hobbs, C. Dyer, M. Ghuman, F. J. Hughes, *J. Periodontal Res.* **2020**, *55*, 859.
- [92] H. Makkar, S. Atkuru, Y. L. Tang, T. Sethi, C. T. Lim, K. S. Tan, G. Sriram, *J. Tissue Eng.* **2022**, *13*, 204173142211116.
- [93] L. Bierbaumer, U. Y. Schwarze, R. Gruber, W. Neuhaus, *Tissue Barriers* **2018**, *6*, 1479568.
- [94] G. N. Belibasakis, T. Thurnheer, N. Bostanci, *PLoS One* **2013**, *8*, e81581.
- [95] J. K. Buskermolen, M. M. Janus, S. Roffel, B. P. Krom, S. Gibbs, *J. Dent. Res.* **2018**, *97*, 201.
- [96] S. Hu, G. Muniraj, A. Mishra, K. Hong, J. L. Lum, C. H. L. Hong, V. Rosa, G. Sriram, *Dent. Mater.* **2022**, *38*, 1385.
- [97] M. Sahle, M. Wachendorfer, A. L. Palkowitz, R. Nasehi, S. Aveic, H. Fischer, *Macromol. Biosci.* **2023**, e2300162.
- [98] T. Iwayama, H. Sakashita, M. Takedachi, S. Murakami, *Jpn. Dent. Sci. Rev.* **2022**, *58*, 172.
- [99] M. E. Grawish, *World J. Stem Cells* **2018**, *10*, 116.
- [100] L. Fonticoli, Y. Della Rocca, T. S. Rajan, G. Murmura, O. Trubiani, S. Oliva, J. Pizzicannella, G. D. Marconi, F. Diomedede, *Int. J. Mol. Sci.* **2022**, *23*.
- [101] N. Buduneli, *Biomarkers Periodontal Health Disease* **2020**, *1*.
- [102] N. H. Mohd Nor, Z. Berahim, A. Ahmad, T. P. Kannan, *Curr. Stem Cell Res. Ther.* **2017**, *12*, 52.
- [103] L. Moroni, J. A. Burdick, C. Highley, S. J. Lee, Y. Morimoto, S. Takeuchi, J. J. Yoo, *Nat. Rev. Mater.* **2018**, *3*, 21.
- [104] J. Beigel, K. Fella, P. J. Kramer, M. Kroeger, P. Hewitt, *Toxicol. In Vitro* **2008**, *22*, 171.
- [105] J. M. Polak, A. E. Bishop, *Ann. N. Y. Acad. Sci.* **2006**, *1068*, 352.
- [106] H. A. Nielsen, *Ugeskr. Laeger.* **1977**, *139*, 3011.
- [107] H. M. Nielsen, J. C. Verhoef, M. Ponec, M. R. Rassing, *J. Control. Release* **1999**, *60*, 223.
- [108] Y. Wang, Z. Zuo, K. K. Lee, M. S. Chow, *Int. J. Pharm.* **2007**, *334*, 27.
- [109] J. Jacobsen, E. B. Nielsen, K. Brondum-Nielsen, M. E. Christensen, H. B. Olin, N. Tommerup, M. R. Rassing, *Eur. J. Oral Sci.* **1999**, *107*, 138.
- [110] C. T. Dickman, R. Towle, R. Saini, C. Garnis, *J. Oral Pathol. Med.* **2015**, *44*, 329.
- [111] J. K. Buskermolen, C. M. Reijnders, S. W. Spiekstra, T. Steinberg, C. J. Kleverlaan, A. J. Feilzer, A. D. Bakker, S. Gibbs, *Tissue Eng., Part C: Methods* **2016**, *22*, 781.
- [112] D. Hare, S. Collins, B. Cuddington, K. Mossman, *Viruses* **2016**, *8*, 297.
- [113] C. D. Toouli, L. I. Huschtscha, A. A. Neumann, J. R. Noble, L. M. Colgin, B. Hukku, R. R. Reddel, *Oncogene* **2002**, *21*, 128.
- [114] L. Shang, D. Deng, J. K. Buskermolen, S. Roffel, M. M. Janus, B. P. Krom, W. Crielard, S. Gibbs, *Front. Cell Infect. Microbiol.* **2019**, *9*, 282.
- [115] P. L. Wang, M. Oido-Mori, T. Fujii, Y. Kowashi, M. Kikuchi, Y. Suetsugu, J. Tanaka, Y. Azuma, M. Shinohara, K. Ohura, *Biochem. Biophys. Res. Commun.* **2001**, *288*, 863.
- [116] P. C. Lekic, N. Pender, C. A. McCulloch, *Crit. Rev. Oral Biol. Med.* **1997**, *8*, 253.
- [117] D. W. Williams, T. Greenwell-Wild, L. Brenchley, N. Dutzan, A. Overmiller, A. P. Sawaya, S. Webb, D. Martin, N. N. Genomics, C. Computational Biology, G. Hajishengallis, K. Divaris, M. Morasso, M. Haniffa, N. M. Moutsopoulos, *Cell* **2021**, *184*, 4090.
- [118] P. Kaur, V. Kakar, *Int. J. Sci. Res.* **2014**, *3*, 2012.
- [119] F. J. Schoen, R. N. Mitchell, *Biomaterials Science*, Elsevier, Amsterdam **2013**.
- [120] H. Vindin, S. M. Mithieux, A. S. Weiss, *Matrix Biol.* **2019**, *84*, 4.
- [121] C. C. Hughes, *Curr. Opin. Hematol.* **2008**, *15*, 204.
- [122] P. C. Smith, C. Martinez, J. Martinez, C. A. McCulloch, *Front. Physiol.* **2019**, *10*, 270.
- [123] H. Makkar, C. T. Lim, K. S. Tan, G. Sriram, *Biofabrication* **2023**, *15*.
- [124] S. Atkuru, G. Muniraj, T. Sudhaharan, K. H. Chiam, G. D. Wright, G. Sriram, *J. Periodontal Res.* **2021**, *56*, 108.
- [125] J. J. Kim, L. Hou, N. F. Huang, *Acta Biomater.* **2016**, *41*, 17.
- [126] K. A. Cabral, V. Srivastava, A. J. Graham, M. C. Coyle, C. Stashko, V. Weaver, Z. J. Gartner, *Tissue Eng., Part A* **2023**, *29*, 80.
- [127] G. Sriram, H. K. Handral, S. U. Gan, I. Islam, A. J. Rufaihah, T. Cao, *Biofabrication* **2020**, *12*, 045015.
- [128] A. A. Szklanny, M. Machour, I. Redenski, V. Chochola, I. Goldfracht, B. Kaplan, M. Epshtein, H. Simaan Yameen, U. Merdler, A. Feinberg, D. Seliktar, N. Korin, J. Jaros, S. Levenberg, *Adv. Mater.* **2021**, *33*, 2102661.
- [129] S. Muthusamy, S. Kannan, M. Lee, V. Sanjairaj, W. F. Lu, J. Y. H. Fuh, G. Sriram, T. Cao, *Biotechnol. Bioeng.* **2021**, *118*, 3150.
- [130] J. Nulty, F. E. Freeman, D. C. Browe, R. Burdis, D. P. Ahern, P. Pitacco, Y. B. Lee, E. Alsberg, D. J. Kelly, *Acta Biomater.* **2021**, *126*, 154.
- [131] K. Ronaldson-Bouchard, D. Teles, K. Yeager, D. N. Tavakol, Y. Zhao, A. Chramiec, S. Tagore, M. Summers, S. Stylianos, M. Tamargo, B. M. Lee, S. P. Halligan, E. H. Abaci, Z. Guo, J. Jackow, A. Pappalardo, J. Shih, R. K. Soni, S. Sonar, C. German, A. M. Christiano, A. Califano, K. K. Hirschi, C. S. Chen, A. Przekwas, G. Vunjak-Novakovic, *Nat. Biomed. Eng.* **2022**, *6*, 351.

- [132] S. Kim, H. Lee, M. Chung, N. L. Jeon, *Lab Chip* **2013**, *13*, 1489.
- [133] D. B. Kolesky, R. L. Truby, A. S. Gladman, T. A. Busbee, K. A. Homan, J. A. Lewis, *Adv. Mater.* **2014**, *26*, 3124.
- [134] E. A. Margolis, D. S. Cleveland, Y. P. Kong, J. A. Beamish, W. Y. Wang, B. M. Baker, A. J. Putnam, *Lab Chip* **2021**, *21*, 1150.
- [135] J. S. Jeon, S. Bersini, J. A. Whisler, M. B. Chen, G. Dubini, J. L. Charest, M. Moretti, R. D. Kamm, *Integr. Biol.* **2014**, *6*, 555.
- [136] C. M. Ghajar, K. S. Blevins, C. C. Hughes, S. C. George, A. J. Putnam, *Tissue Eng.* **2006**, *12*, 2875.
- [137] A. L. Gard, R. J. Luu, R. Maloney, M. H. Cooper, B. P. Cain, H. Azizgolshani, B. C. Isenberg, J. T. Borenstein, J. Ong, J. L. Charest, E. M. Vedula, *Commun. Biol.* **2023**, *6*, 92.
- [138] D. S. Masson-Meyers, L. E. Bertassoni, L. Tayebi, *Connect. Tissue Res.* **2022**, *63*, 514.
- [139] K. Nishiyama, T. Akagi, S. Iwai, M. Akashi, *Tissue Eng., Part C: Methods* **2019**, *25*, 262.
- [140] M. Heller, E. V. Frerick-Ochs, H. K. Bauer, E. Schiegnitz, D. Flesch, J. Brieger, R. Stein, B. Al-Nawas, C. Brochhausen, J. W. Thuroff, R. E. Unger, W. Brenner, *Biomaterials* **2016**, *77*, 207.
- [141] B. Mikecs, J. Vag, G. Gerber, B. Molnar, G. Feigl, A. Shahbazi, *BMC Oral Health* **2021**, *21*, 160.
- [142] S. Perotto, F. Romano, L. Cricenti, S. Gotti, M. Aimetti, *Int. J. Periodont. Restor. Dent.* **2017**, *37*, 551.
- [143] N. M. Le, S. Song, H. Zhou, J. Xu, Y. Li, C. E. Sung, A. Sadr, K. H. Chung, H. M. Subhash, L. Kilpatrick, R. K. Wang, *J. Biophoton.* **2018**, *11*, e201800242.
- [144] S. Yoshida, K. Noguchi, K. Imura, Y. Miwa, M. Sunohara, I. Sato, *Okajimas Folia Anat. Jpn.* **2011**, *88*, 103.
- [145] E. Molnar, B. Molnar, Z. Lohinai, Z. Toth, Z. Benyo, L. Hricisak, P. Windisch, J. Vag, *Biomed Res. Int.* **2017**, *2017*, 1.
- [146] K. Banerjee, J. Radhakrishnan, N. Ayyadurai, P. Ganesan, N. R. Kamini, *J. Sci.: Adv. Mater. Dev.* **2022**, *7*, 100491.
- [147] I. Calejo, R. Costa-Almeida, M. E. Gomes, *Adv. Exp. Med. Biol.* **2019**, *1144*, 71.
- [148] S. Patel, J. M. Caldwell, S. B. Doty, W. N. Levine, S. Rodeo, L. J. Soslowsky, S. Thomopoulos, H. H. Lu, *J. Orthop. Res.* **2018**, *36*, 1069.
- [149] M. Rahimnejad, R. Rezvaninejad, R. Rezvaninejad, R. Franca, *Biomed. Phys. Eng. Express* **2021**, *7*, 062001.
- [150] M. Rahimnejad, C. Charbonneau, Z. He, S. Lerouge, *J. Biomed. Mater. Res. A* **2023**, *111*, 1031.
- [151] A. Soroushanova, L. M. Delgado, Z. Wu, N. Shologu, A. Kshirsagar, R. Raghunath, A. M. Mullen, Y. Bayon, A. Pandit, M. Raghunath, D. I. Zeugolis, *Adv. Mater.* **2019**, *31*, 1801651.
- [152] J. D. San Antonio, O. Jacenko, A. Fertala, J. Orgel, *Bioengineering* **2020**, *8*, 3.
- [153] E. M. Green, J. C. Mansfield, J. S. Bell, C. P. Winlove, *Interface Focus* **2014**, *4*, 20130058.
- [154] X. Xu, S. Ren, L. Li, Y. Zhou, W. Peng, Y. Xu, *J. Biomater. Appl.* **2021**, *36*, 55.
- [155] J. A. Reid, A. McDonald, A. Callanan, *PLoS One* **2020**, *15*, e0240332.
- [156] M. R. Ramezani, Z. Ansari-Asl, E. Hoveizi, A. R. Kiasat, *Mater. Chem. Phys.* **2019**, *229*, 242.
- [157] D. G. Han, C. B. Ahn, J. H. Lee, Y. Hwang, J. H. Kim, K. Y. Park, J. W. Lee, K. H. Son, *Polymers* **2019**, *11*, 643.
- [158] A. Daghreery, J. A. Ferreira, I. J. de Souza Araujo, B. H. Clarkson, G. J. Eckert, S. B. Bhaduri, J. Malda, M. C. Bottino, *Adv. Healthcare Mater.* **2021**, *10*, e2101152.
- [159] A. Mathur, O. P. Kharbanda, V. Koul, A. K. Dinda, M. F. Anwar, S. Singh, *J. Periodontol.* **2022**, *93*, 1578.
- [160] N. Abedi, N. Rajabi, M. Kharazilha, F. Nejatidansh, L. Tayebi, *J. Oral Biol. Craniofac. Res.* **2022**, *12*, 782.
- [161] P. Zhao, W. Chen, Z. Feng, Y. Liu, P. Liu, Y. Xie, D. G. Yu, *Int. J. Nanomed.* **2022**, *17*, 4137.
- [162] S. Hong, B. Y. Jung, C. Hwang, *Tissue Eng. Regen. Med.* **2017**, *14*, 371.
- [163] V. Flores, B. Venegas, W. Donoso, C. Ulloa, A. Chaparro, V. Sousa, V. Beltran, *Int. J. Environ. Res. Public Health* **2022**, *19*, 8388.
- [164] H. Dan, C. Vaquette, A. G. Fisher, S. M. Hamlet, Y. Xiao, D. W. Huttmacher, S. Ivanovski, *Biomaterials* **2014**, *35*, 113.
- [165] C. Vaquette, J. Cooper-White, *Acta Biomater.* **2013**, *9*, 4599.
- [166] S. D. McCullen, P. R. Miller, S. D. Gittard, R. E. Gorga, B. Pourdeyhimi, R. J. Narayan, E. G. Lobo, *Tissue Eng., Part C: Methods* **2010**, *16*, 1095.
- [167] J. Li, M. Chen, X. Wei, Y. Hao, J. Wang, *Materials* **2017**, *10*, 831.
- [168] C. Y. Wang, Y. C. Chiu, A. K. Lee, Y. A. Lin, P. Y. Lin, M. Y. Shie, *Biomedicines* **2021**, *9*, 431.
- [169] D. M. Dos Santos, S. R. de Annunzio, J. C. Carmello, A. C. Pavarina, C. R. Fontana, D. S. Correa, *ACS Appl. Biol. Mater.* **2022**, *5*, 146.
- [170] C. H. Park, H. F. Rios, Q. Jin, J. V. Sugai, M. Padiol-Molina, A. D. Taut, C. L. Flanagan, S. J. Hollister, W. V. Giannobile, *Biomaterials* **2012**, *33*, 137.
- [171] C. H. Park, H. F. Rios, Q. Jin, M. E. Bland, C. L. Flanagan, S. J. Hollister, W. V. Giannobile, *Biomaterials* **2010**, *31*, 5945.
- [172] C. H. Park, H. F. Rios, A. D. Taut, M. Padiol-Molina, C. L. Flanagan, S. P. Pilipchuk, S. J. Hollister, W. V. Giannobile, *Tissue Eng., Part C: Methods* **2014**, *20*, 533.
- [173] C. H. Lee, J. Hajibandeh, T. Suzuki, A. Fan, P. Shang, J. J. Mao, *Tissue Eng., Part A* **2014**, *20*, 1342.
- [174] Y. C. Chou, D. Lee, T. M. Chang, Y. H. Hsu, Y. H. Yu, S. J. Liu, S. W. N. Ueng, *Int. J. Mol. Sci.* **2016**, *17*, 595.
- [175] I. Zein, D. W. Huttmacher, K. C. Tan, S. H. Teoh, *Biomaterials* **2002**, *23*, 1169.
- [176] N. A. S. M. Pu'ad, R. H. A. Haq, H. M. Noh, H. Z. Abdullah, M. I. Idris, T. C. Lee, *Mater. Today Proc.* **2020**, *29*, 228.
- [177] Q. Chen, J. D. Mangadlao, J. Wallat, A. De Leon, J. K. Pokorski, R. C. Advincula, *ACS Appl. Mater. Interfaces* **2017**, *9*, 4015.
- [178] E. M. Goncalves, F. J. Oliveira, R. F. Silva, M. A. Neto, M. H. Fernandes, M. Amaral, M. Vallet-Regí, M. Vila, *J. Biomed. Mater. Res., Part B* **2016**, *104*, 1210.
- [179] D. H. Go, Y. K. Joung, S. Y. Park, Y. D. Park, K. D. Park, *J. Biomed. Mater. Res. A* **2008**, *86*, 842.
- [180] P. D. Dalton, C. Vaquette, B. L. Farrugia, T. R. Dargaville, T. D. Brown, D. W. Huttmacher, *Biomater. Sci.* **2013**, *1*, 171.
- [181] H. Li, Y. Xu, H. Xu, J. Chang, *J. Mater. Chem. B* **2014**, *2*, 5492.
- [182] D. Gao, Z. Wang, Z. Wu, M. Guo, Y. Wang, Z. Gao, P. Zhang, Y. Ito, *Mater. Sci. Eng., C: Mater. Biol. Appl.* **2020**, *112*, 110942.
- [183] W. Aljohani, M. W. Ullah, X. Zhang, G. Yang, *Int. J. Biol. Macromol.* **2018**, *107*, 261.
- [184] A. C. Daly, M. E. Prendergast, A. J. Hughes, J. A. Burdick, *Cell* **2021**, *184*, 18.
- [185] R. França, J. Winkler, H. H. Hsu, M. Rahimnejad, Z. Abdali, in *Dental Biomaterials*, World Scientific, Singapore **2019**.
- [186] X. Li, B. Liu, B. Pei, J. Chen, D. Zhou, J. Peng, X. Zhang, W. Jia, T. Xu, *Chem. Rev.* **2020**, *120*, 10793.
- [187] C. Mangano, B. Barboni, L. Valbonetti, P. Berardinelli, A. Martelli, A. Muttini, R. Bedini, S. Tete, A. Piattelli, M. Mattioli, *J. Oral Implantol.* **2015**, *41*, 240.
- [188] K. Kim, C. H. Lee, B. K. Kim, J. J. Mao, *J. Dent. Res.* **2010**, *89*, 842.
- [189] J. Adhikari, A. Roy, A. Chanda, A. G. D. S. Thomas, M. Ghosh, J. Kim, P. Saha, *Biomater. Sci.* **2023**, *11*, 1236.
- [190] V. Lee, G. Singh, J. P. Trasatti, C. Bjornsson, X. Xu, T. N. Tran, S. S. Yoo, G. Dai, P. Karande, *Tissue Eng., Part C: Methods* **2014**, *20*, 473.
- [191] S. Michael, H. Sorg, C. T. Peck, L. Koch, A. Deiwick, B. Chichkov, P. M. Vogt, K. Reimers, *PLoS One* **2013**, *8*, e57741.
- [192] L. Ge, L. L. Yang, R. Bron, J. K. Burgess, P. van Rijn, *ACS Appl. Bio Mater.* **2020**, *3*, 2104.

- [193] D. Cheng, R. K. Jayne, A. Tamborini, J. Eyckmans, A. E. White, C. S. Chen, *Biofabrication* **2019**, *11*, 021001.
- [194] B. Zhang, J. Huang, R. J. Narayan, *J. Mater. Chem. B* **2020**, *8*, 8149.
- [195] P. Giachini, S. S. Gupta, W. Wang, D. Wood, M. Yunusa, E. Baharlou, M. Sitti, A. Menges, *Sci. Adv.* **2020**, *6*, eaay0929.
- [196] M. Hu, F. Jia, W. P. Huang, X. Li, D. F. Hu, J. Wang, K. F. Ren, G. S. Fu, Y. B. Wang, J. Ji, *Bioact. Mater.* **2021**, *6*, 1413.
- [197] A. M. Loye, E. R. Kinser, S. Bensouda, M. Shayan, R. Davis, R. Wang, Z. Chen, U. D. Schwarz, J. Schroers, T. R. Kyriakides, *Sci. Rep.* **2018**, *8*, 8758.
- [198] C. A. Kraynak, D. J. Yan, L. J. Suggs, *Acta Biomater.* **2020**, *108*, 250.
- [199] T. De Ryck, C. Grootaert, L. Jaspaert, F. M. Kerckhof, M. Van Gele, J. De Schrijver, P. Van den Abbeele, S. Swift, M. Bracke, T. Van de Wiele, B. Vanhoecle, *Appl. Microbiol. Biotechnol.* **2014**, *98*, 6831.
- [200] S. N. Bhatia, D. E. Ingber, *Nat. Biotechnol.* **2014**, *32*, 760.
- [201] C. M. Franca, G. S. Balbinot, D. Cunha, V. P. A. Saboia, J. Ferracane, L. E. Bertassoni, *Acta Biomater.* **2022**, *150*, 58.
- [202] L. Jin, N. Kou, F. An, Z. Gao, T. Tian, J. Hui, C. Chen, G. Ma, H. Mao, H. Liu, *Biosensors* **2022**, *12*.
- [203] C. M. Franca, A. Tahayeri, N. S. Rodrigues, S. Ferdosian, R. M. Puppini Rontani, G. Sereda, J. L. Ferracane, L. E. Bertassoni, *Lab Chip* **2020**, *20*, 405.
- [204] N. S. Rodrigues, C. M. Franca, A. Tahayeri, Z. Ren, V. P. A. Saboia, A. J. Smith, J. L. Ferracane, H. Koo, L. E. Bertassoni, *J. Dent. Res.* **2021**, *100*, 1136.
- [205] K. Bao, G. N. Belibasakis, N. Selevsek, J. Grossmann, N. Bostanci, *Sci. Rep.* **2015**, *5*, 15999.
- [206] K. Bao, A. Papadimitropoulos, B. Akgul, G. N. Belibasakis, N. Bostanci, *Virulence* **2015**, *6*, 265.
- [207] K. L. Ly, X. Luo, C. B. Raub, *Biofabrication* **2022**, *15*.
- [208] C. Rahimi, B. Rahimi, D. Padova, S. A. Rooholghodos, D. R. Bienek, X. Luo, G. Kaufman, C. B. Raub, *Biomicrofluidics* **2018**, *12*, 054106.
- [209] J. J. Koning, C. T. Rodrigues Neves, K. Schimek, M. Thon, S. W. Spiekstra, T. Waaijman, T. D. de Gruijl, S. Gibbs, *Front. Toxicol.* **2021**, *3*, 824825.
- [210] K. L. Ly, S. A. Rooholghodos, C. Rahimi, B. Rahimi, D. R. Bienek, G. Kaufman, C. B. Raub, X. Luo, *Biomed. Microdevices* **2021**, *23*, 7.
- [211] J. W. Cheung, E. E. Rose, J. P. Santerre, *Acta Biomater.* **2013**, *9*, 6867.
- [212] F. A. Navarro, S. Mizuno, J. C. Huertas, J. Glowacki, D. P. Orgill, *Wound Repair Regen.* **2001**, *9*, 507.
- [213] E. J. Lee, Y. Kim, P. Salipante, A. P. Kotula, S. Lipshutz, D. T. Graves, S. Alimperti, *Bioengineering* **2023**, *10*, 517.
- [214] M. Adelfio, M. Bonzanni, G. E. Callen, B. J. Paster, H. Hasturk, C. E. Ghezzi, *Acta Biomater.* **2023**, *167*, 321.
- [215] A. Ravichandran, Y. Liu, S. H. Teoh, *J. Tissue Eng. Regen. Med.* **2018**, *12*, e7.
- [216] C. L. Simpson, D. M. Patel, K. J. Green, *Nat. Rev. Mol. Cell Biol.* **2011**, *12*, 565.
- [217] C. J. Smith, E. K. Parkinson, J. Yang, J. Pratten, E. A. O'Toole, M. P. Caley, K. M. Braun, *J. Dent.* **2022**, *125*, 104251.
- [218] D. Pereira, I. Sequeira, *Front. Cell Dev. Biol.* **2021**, *9*, 682143.
- [219] M. Waasdorp, B. P. Krom, F. J. Bikker, P. P. M. van Zuijlen, F. B. Niessen, S. Gibbs, *Biomolecules* **2021**, *11*, 1165.
- [220] L. Vitkov, J. Singh, C. Schauer, B. Minnich, J. Kronic, H. Oberthaler, S. Gamsjaeger, M. Herrmann, J. Knopf, M. Hannig, *Int. J. Mol. Sci.* **2023**, *24*, 4544.
- [221] A. Herman, A. P. Herman, *Skin Res. Technol.* **2019**, *25*, 111.
- [222] A. M. Szpaderska, C. G. Walsh, M. J. Steinberg, L. A. DiPietro, *J. Dent. Res.* **2005**, *84*, 309.
- [223] A. M. Szpaderska, J. D. Zuckerman, L. A. DiPietro, *J. Dent. Res.* **2003**, *82*, 621.
- [224] D. B. Shannon, S. T. McKeown, F. T. Lundy, C. R. Irwin, *Wound Repair Regen.* **2006**, *14*, 172.
- [225] P. Stephens, K. J. Davies, N. Occeleston, R. D. Pleass, C. Kon, J. Daniels, P. T. Khaw, D. W. Thomas, *Br. J. Dermatol.* **2001**, *144*, 229.
- [226] J. Ma, C. Qin, J. Wu, H. Zhang, H. Zhuang, M. Zhang, Z. Zhang, L. Ma, X. Wang, B. Ma, J. Chang, C. Wu, *Adv. Healthcare Mater.* **2021**, *10*, e2100523.
- [227] T. Baltazar, J. Merola, C. Catarino, C. B. Xie, N. C. Kirkiles-Smith, V. Lee, S. Hotta, G. Dai, X. Xu, F. C. Ferreira, W. M. Saltzman, J. S. Pober, P. Karande, *Tissue Eng., Part A* **2020**, *26*, 227.
- [228] B. S. Kim, Y. W. Kwon, J. S. Kong, G. T. Park, G. Gao, W. Han, M. B. Kim, H. Lee, J. H. Kim, D. W. Cho, *Biomaterials* **2018**, *168*, 38.
- [229] A. M. Jorgensen, M. Varkey, A. Gorkun, C. Clouse, L. Xu, Z. Chou, S. V. Murphy, J. Molnar, S. J. Lee, J. J. Yoo, S. Soker, A. Atala, *Tissue Eng., Part A* **2020**, *26*, 512.
- [230] W. L. Ng, J. T. Z. Qi, W. Y. Yeong, M. W. Naing, *Biofabrication* **2018**, *10*, 025005.
- [231] F. Afghah, M. Ullah, J. Seyyed Monfared Zanjani, P. Akkus Sut, O. Sen, M. Emanet, B. Saner Okan, M. Culha, Y. Menciloglu, M. Yildiz, B. Koc, *Biomed. Mater.* **2020**, *15*, 035015.
- [232] G. Sriram, M. Alberti, Y. Dancik, B. Wu, R. G. Wu, Z. X. Feng, S. Ramasamy, P. L. Bigliardi, M. Bigliardi-Qi, Z. P. Wang, *Mater. Today* **2018**, *21*, 326.
- [233] Y. Dancik, G. Sriram, B. Rout, Y. Zou, M. Bigliardi-Qi, P. L. Bigliardi, *Analyst* **2018**, *143*, 1065.
- [234] R. Marks, *J. Nutr.* **2004**, *134*, 2017S.
- [235] N. Bostanci, G. N. Belibasakis, *Periodontol 2000* **2018**, *76*, 68.
- [236] K. Derr, J. Zou, K. Luo, M. J. Song, G. S. Sittampalam, C. Zhou, S. Michael, M. Ferrer, P. Derr, *Tissue Eng., Part C: Methods* **2019**, *25*, 334.
- [237] E. Ilhan, S. Cesur, E. Guler, F. Topal, D. Albayrak, M. M. Guncu, M. E. Cam, T. Taskin, H. T. Sasmazel, B. Aksu, F. N. Oktar, O. Gunduz, *Int. J. Biol. Macromol.* **2020**, *161*, 1040.
- [238] L. J. Pourchet, A. Thepot, M. Albouy, E. J. Courtial, A. Boher, L. J. Blum, C. A. Marquette, *Adv. Healthcare Mater.* **2017**, *6*, 1601101.
- [239] S. Madiedo-Podvrsan, J.-P. Belaïdi, S. Desbouis, L. Simonetti, Y. Ben-Khalifa, C. Collin-Djangone, J. Soeur, M. Rielland, *Sci. Rep.* **2021**, *11*, 6217.
- [240] D. Min, W. Lee, I. H. Bae, T. R. Lee, P. Croce, S. S. Yoo, *Exp. Dermatol.* **2018**, *27*, 453.
- [241] M. Albanna, K. W. Binder, S. V. Murphy, J. Kim, S. A. Qasem, W. Zhao, J. Tan, I. B. El-Amin, D. D. Dice, J. Marco, J. Green, T. Xu, A. Skardal, J. H. Holmes, J. D. Jackson, A. Atala, J. J. Yoo, *Sci. Rep.* **2019**, *9*, 1856.
- [242] A. Bozkurt, K. Kose, J. Coll-Font, C. Alessi-Fox, D. H. Brooks, J. G. Dy, M. Rajadhyaksha, *Sci. Rep.* **2021**, *11*, 12576.
- [243] H. A. El Madani, E. Tancrede-Bohin, A. Bensussan, A. Colonna, A. Dupuy, M. Bagot, A. M. Pena, *J. Biomed. Opt.* **2012**, *17*, 026009.
- [244] M. J. Koehler, K. Konig, P. Elsner, R. Buckle, M. Kaatz, *Opt. Lett.* **2006**, *31*, 2879.
- [245] M. Lee, S. Kannan, G. Muniraj, V. Rosa, W. F. Lu, J. Y. H. Fuh, G. Sriram, T. Cao, *Tissue Eng., Part B: Rev.* **2022**, *28*, 926.
- [246] F. D. Fleischli, S. Mathes, C. Adhart, *Vib. Spectrosc.* **2013**, *68*, 29.
- [247] M. G. Tosato, D. E. Orallo, S. M. Ali, M. S. Churio, A. A. Martin, L. Dixelio, *J. Photochem. Photobiol. B* **2015**, *153*, 51.
- [248] S. Abadie, C. Jarde, J. Colombelli, B. Chaput, A. David, J. L. Grolleau, P. Bedos, V. Lobjois, P. Descargues, J. Rouquette, *Skin Res. Technol.* **2018**, *24*, 294.
- [249] K. Kajiya, R. Bise, C. Commerford, I. Sato, T. Yamashita, M. Detmar, *J. Dermatol. Sci.* **2018**, *92*, 3.
- [250] R. M. Martínez-Ojeda, M. D. Pérez-Cárceles, L. C. Ardelean, S. G. Stanciu, J. M. Bueno, *Front. Phys.* **2020**, *8*.
- [251] A. Azaripour, T. Lagerweij, C. Scharbillig, A. E. Jadczyk, B. V. Swaan, M. Molenaar, R. V. Waal, K. Kielbassa, W. Tigchelaar, D. I. Picavet,

- A. Jonker, E. M. L. Hendriks, V. V. V. Hira, M. Khurshed, C. Noorden, *Sci. Rep.* **2018**, *8*, 1647.
- [252] L. Y. Daikuara, X. Chen, Z. Yue, D. Skropeta, F. M. Wood, M. W. Fear, G. G. Wallace, *Adv. Funct. Mater.* **2022**, *32*, 2105080.
- [253] T. Steinberg, M. P. Dieterle, P. Tomakidi, *Int. J. Mol. Sci.* **2022**, *23*, 5288.
- [254] B. N. Allen, Q. Wang, Y. Filali, K. S. Worthington, D. S. F. Kacmarynski, *Tissue Eng., Part B: Rev.* **2022**, *28*, 813.
- [255] L.-G. Dai, N.-T. Dai, T.-Y. Chen, L.-Y. Kang, S.-h. Hsu, *Int. J. Bioprint.* **2022**, *28*, e00237.
- [256] J. Dias-Ferreira, M. Teixeira, P. Severino, P. Boonme, J. Jovanovic, A. Zielińska, E. B. Souto, in *Nanotechnol. Tissue Eng. Regener. Med.*, Elsevier, Amsterdam **2023**.
- [257] M. A. Boink, L. J. van den Broek, S. Roffel, K. Nazmi, J. G. Bolscher, A. Gefen, E. C. Veerman, S. Gibbs, *Wound Repair Regen.* **2016**, *24*, 100.



**Maedeh Rahimnejad** earned her doctorate (Ph.D.) in Biomedical Engineering from the University of Montreal, Canada. Presently, she serves as a Postdoctoral Fellow at the School of Dentistry, University of Michigan, USA. Her groundbreaking research focuses on tissue engineering, biomaterials design, and modifications, employing cutting-edge techniques such as bioprinting and nano/microfabrication. Her work holds significant promise in the realms of regenerative medicine and dentistry, where her innovative approaches seek to revolutionize treatment modalities.



**Hardik Makkar** is an Endodontist and holds a Ph.D. from the National University of Singapore with research focused on alternatives to animal experimentation in understanding oral host-microbe interaction using 3D cultures and organ-on-chip systems. He is currently working as a postdoctoral fellow at the School of Dental Medicine, University of Pennsylvania, where his research is aimed at understanding the mechanobiology of fibrotic niches and mechanical regulation of inflammation.



**Renan Dal Fabbro** is a Postdoctoral Fellow at the University of Michigan School of Dentistry. He works in dental tissue regeneration and has expertise in periodontal and periapical diseases, inflammation, and assessing treatments for oral-related conditions. He focuses on developing innovative biomaterials tailored for oral health, bridging research with practical applications using preclinical animal models for clinical relevance.



**Jos Malda** is Professor of Biofabrication in Translational Regenerative Medicine at Utrecht University. He is Head of Research at the Department of Orthopaedics (UMC Utrecht), and he holds a Ph.D. degree from the University of Twente (NL). He is the Past President of the International Society for Biofabrication (ISBF; 2014-2018) and one of the initiators of the first international master's program in Biofabrication. Currently, he is the 2<sup>nd</sup> Vice President of the International Cartilage Regeneration and Joint Preservation Society (ICRS). His research interests include biofabrication technology and materials for orthopaedic regenerative medicine.



**Gopu Sriram** is an Assistant Professor at the Faculty of Dentistry and Department of Biomedical Engineering at the National University of Singapore (NUS). Additionally, he serves as the Co-Thrust Lead at the NUS Centre for Additive Manufacturing, overseeing the utilization of biofabrication technologies for applications in oral healthcare. His multidisciplinary research focuses on the convergence of microfluidics, 3D culture, and 3D printing-based biofabrication technologies for dental and craniofacial research. With a specific emphasis on host-microbe-material interactions, his research aims to deepen the understanding of dental and periodontal health and disease, while also developing novel regenerative strategies to address these challenges.



**Marco C. Bottino** is the Robert W. Browne Endowed Professor of Dentistry in the Department of Cariology, Restorative Sciences, and Endodontics (CRSE) at the University of Michigan School of Dentistry. He is currently the Director of Research in CRSE and the Director of the Postgraduate Program in Regenerative Dentistry. As a principal investigator, Marco has received research grants related to regenerative medicine from the National Institutes of Health (NIH), foundations, and private industry. His research interests include drug delivery, scaffolds for pulp-dentin complex regeneration, personalized scaffolds for craniomaxillofacial bone and periodontal regeneration, and soft tissue reconstruction.